Current-Driven Kink Instability in Magnetically Dominated Relativistic Jets

Yosuke Mizuno
Institute of Astronomy
National Tsing-Hua University

Collaborators
Y. Lyubarsky (Ben-Gurion Univ), P. E. Hardee (Univ. of Alabama),
K.-I. Nishikawa (NSSTC/ Univ. of Alabama in Huntsville)

Mizuno, Lyubarsky, Nishikawa, & Hardee 2009, ApJ, 700, 684
Mizuno, Lyubarsky, Nishikawa, & Hardee 2012, ApJ, 757, 16

Contents

- Introduction of Relativistic Jets
- Introduction of CD Kink Instability
- 3D (G)RMHD Simulation Code RAISHIN
- 3D RMHD Simulations of CD Kink Instability (static plasma column case), magnetic pitch distribution effect
- 3D RMHD Simulations of CD Kink Instability (sub-Alfvenic jet case), jet shear effect
- 3D RMHD Simulations of CD Kink Instability (rotating relativistic jet case), jet flow & rotation effect
- Summery

Contents

- Introduction: Relativistic Jets
- Introduction: Current-Driven Kink Instability
- 3D (G)RMHD Simulation Code RAISHIN
- 3D RMHD Simulations of CD Kink Instability (static plasma column case), magnetic pitch distribution effect
- 3D RMHD Simulations of CD Kink Instability (rotating relativistic jet case), jet flow & rotation effect
- Summery

Relativistic Regime

- Kinetic energy >> rest-mass energy
  - Fluid velocity ~ light speed
  - Lorentz factor $\gamma >> 1$
  - Relativistic jets/ejecta/wind/blast waves (shocks) in AGNs, GRBs, Pulsars
- Thermal energy >> rest-mass energy
  - Plasma temperature >> ion rest mass energy
  - $p/\rho c^2 \sim k_B T/mc^2 >> 1$
  - GRBs, magnetar flare?, Pulsar wind nebulae
- Magnetic energy >> rest-mass energy
  - Magnetization parameter $\sigma >> 1$
  - σ = Poyniting to kinetic energy ratio = $B^2/4\pi\rho c^2\gamma^2$
  - Pulsars magnetosphere, Magnetars
- Gravitational energy >> rest-mass energy
  - $GMm/rmc^2 = r_g/r > 1$
  - Black hole, Neutron star
- Radiation energy >> rest-mass energy
  - $E'_r/\rho c^2 >> 1$
  - Supercritical accretion flow

Relativistic Jets

- *Relativistic jets: outflow of highly collimated plasma*
  - Microquasars, Active Galactic Nuclei, Gamma-Ray Bursts, Jet velocity ～c
  - Generic systems: Compact object（White Dwarf, Neutron Star, Black Hole）+ Accretion Disk

- *Key Issues of Relativistic Jets*
  - Acceleration & Collimation
  - Propagation & Stability

- *Modeling for Jet Production*
  - Magnetohydrodynamics (MHD)
  - Relativity (SR or GR)

- *Modeling of Jet Emission*
  - Particle Acceleration
  - Radiation mechanism

Radio observation of M87 jet

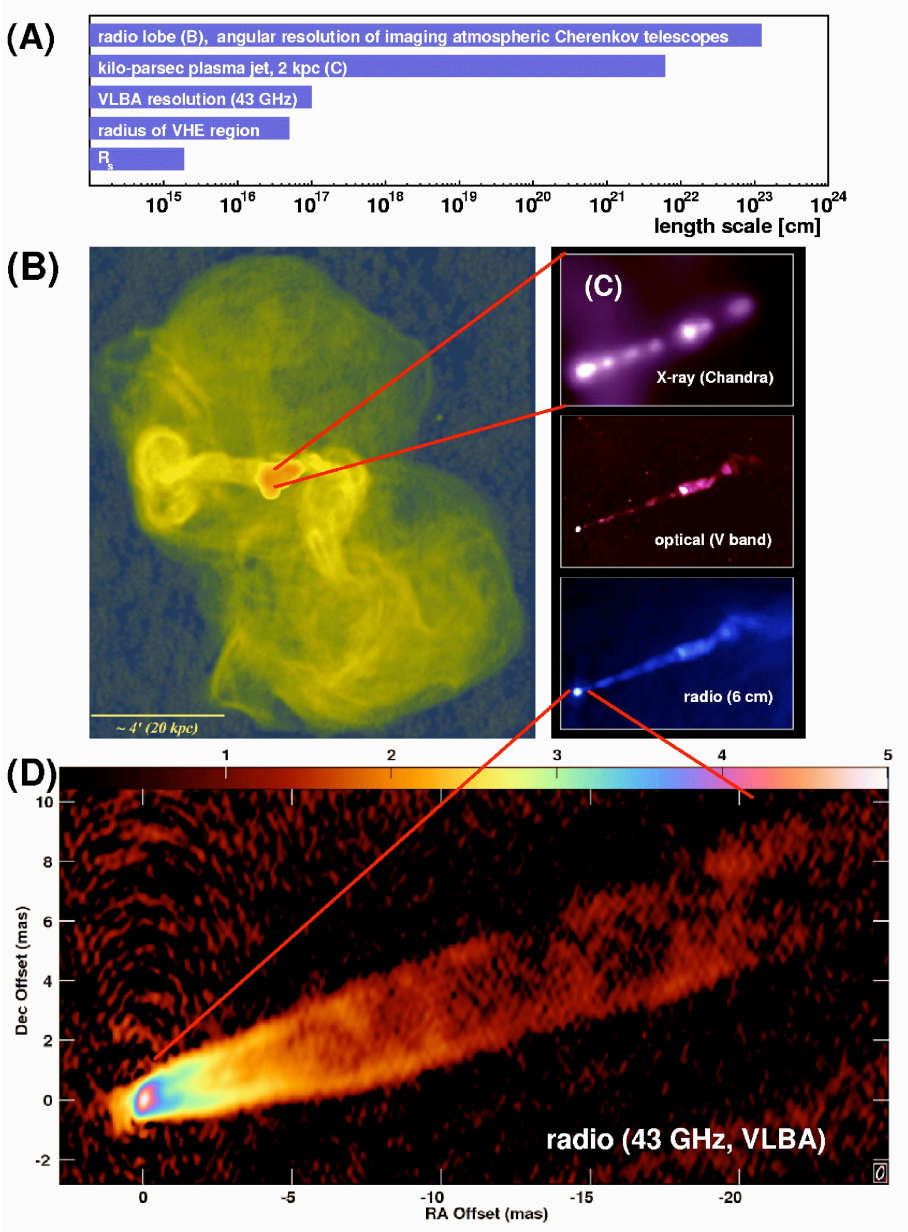

Relativistic Jets in Universe

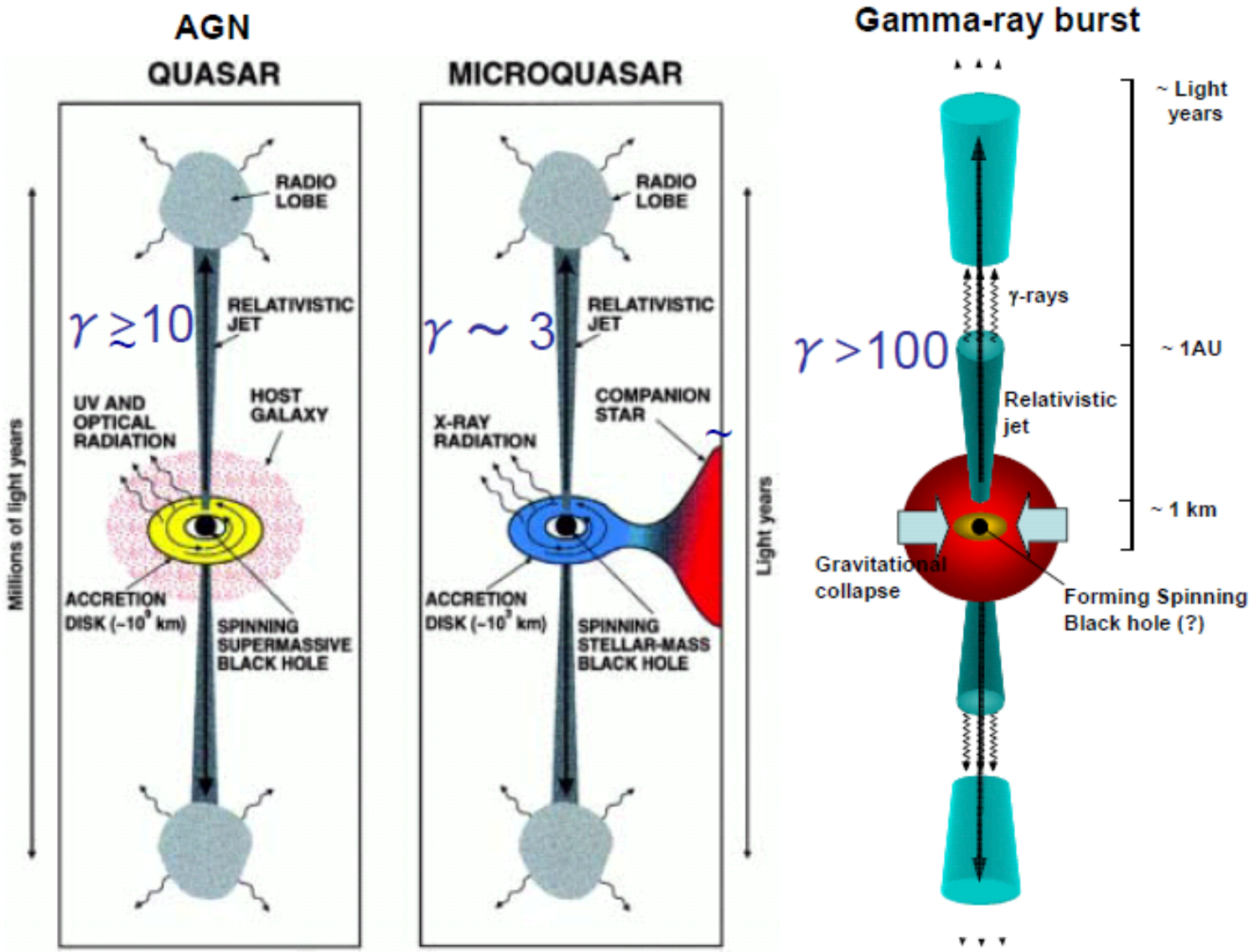

Mirabel & Rodoriguez 1998

Relativistic Jets Formation from GRMHD Simulations

• Many GRMHD simulations of jet formation (e.g., Hawley & Krolik 2006, McKinney 2006, Hardee et al. 2007) suggest that

  • a jet spine (Poynting-flux jet) driven by the magnetic fields threading the ergosphere via MHD process or Blandford-Znajek process

  • may be surrounded by a broad sheath wind driven by the magnetic fields anchored in the accretion disk.

  • High magnetized flow accelerates Γ >>1, but most of energy remains in B field.

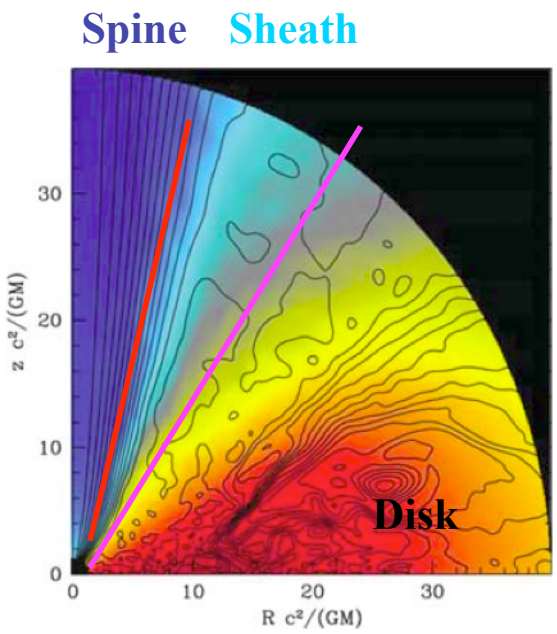

Density distribution (McKinney 2006)

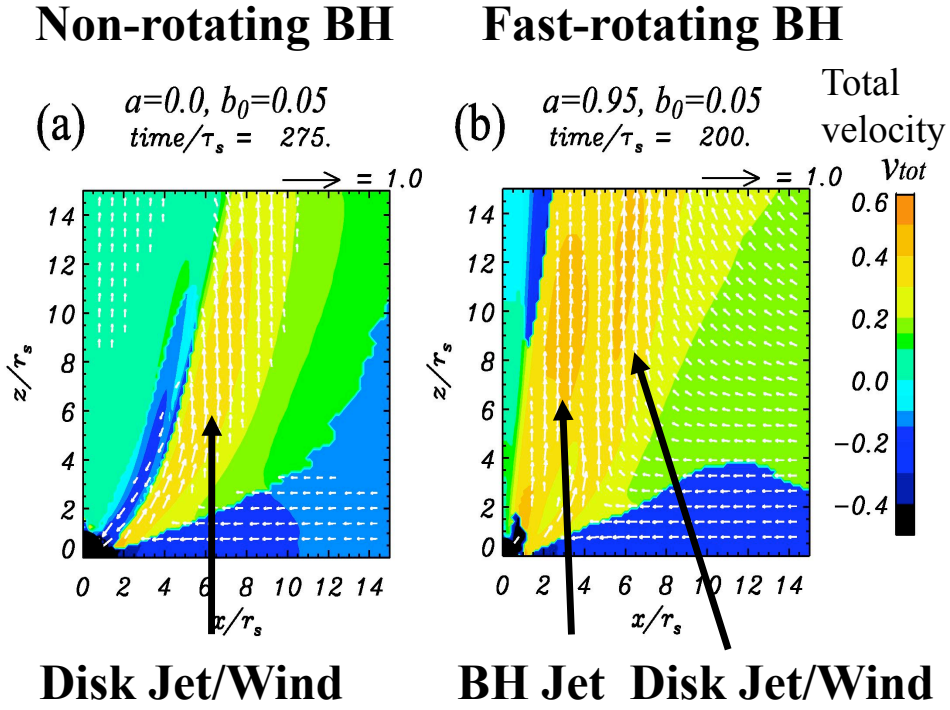

(Hardee, Mizuno & Nishikawa 2007)

M87: Jet Launching & Collimation Region

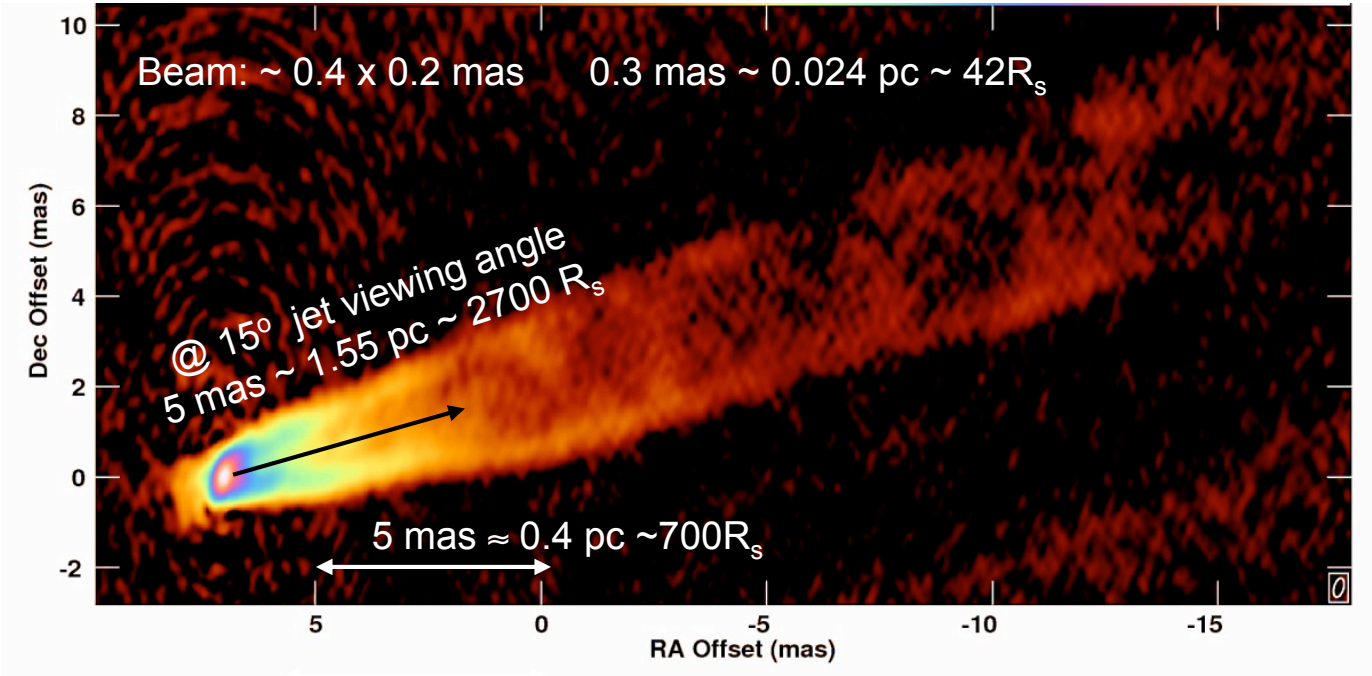

M87:

Walker et al. (2008)

Jet launching region:

$< (0.4 \text{ mas}/\sin 15^0) \sim 200\ R_s$

Jet collimation region:

$\sim (7.5 \text{ mas}/\sin 15^0) \sim 4000\ R_s$

Bulk Lorentz factor: ~ 2 – 3

Blazar Model:

Jorstad et al.(2007)

Bulk Lorentz factor:

$\Gamma \sim 2 - 10$

Particle Lorentz factor:

$\gamma > 10^5$

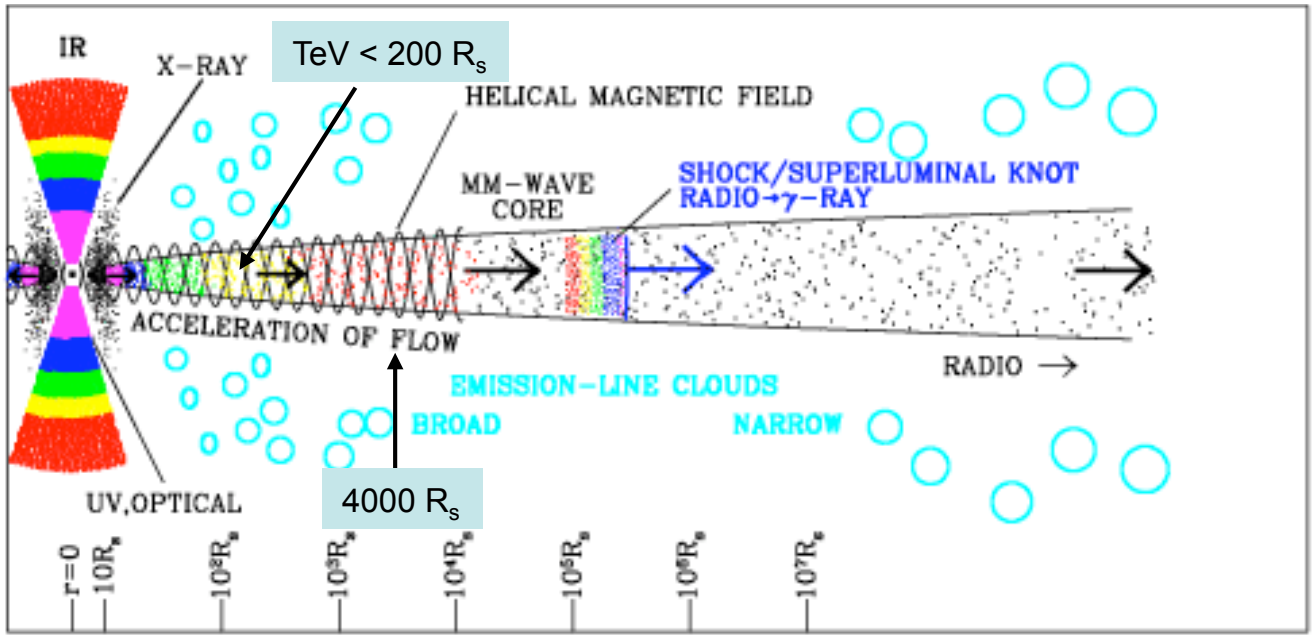

The Five Regions of AGN Jet Propagation

- Hot Spot/Lobe: $\sim 10^9\ r_S$ (~100 kpc; or 20')
  - $\Rightarrow$ Outer jet is *not* Poynting-Flux Dominated
- Kinetic-Flux-Dominated (KFD) Jet: $\sim 10^3 - 10^9\ r_S$
  (0.1 – 10^5 pc; 1 mas – 20')
- Transition Region: $\sim 10^{2.5\pm0.5}\ r_S$ (< 0.1 pc; < 1 mas)
  - Poynting-Flux Dominated (PFD) $\rightarrow$ KFD
- MHD Acceleration/Collimation Region: $\sim 10 - 10^{2.5\pm0.5}\ r_S$
  (1 – < 100 mpc; 10 μas – < 1 mas)
  - The Jet "Nozzle"
- Jet Launching Region: The Accretion Flow; $\sim 5 - 50\ r_S$
  (0.5 – 5 mpc; 5 – 50 μas)
  - Probably unresolved or slightly resolved

Ultra-Fast TeV Flare in Blazars

- Ultra-Fast TeV flares are observed in some Blazars.
- Vary on timescale as sort as

  $t_v \sim 3\text{min} \ll R_s/c \sim 3M_9$ hour
- For the TeV emission to escape pair creation $\Gamma_{em} > 50$ is required (Begelman, Fabian & Rees 2008)
- But PKS 2155-304, Mrk 501 show "moderately" superluminal ejections (v_{app} ~several c)
- Emitter must be compact and extremely fast
- Model for the Fast TeV flaring
  - Internal: Magnetic Reconnection inside jet (Giannios et al. 2009)
  - External: Recollimation shock (Bromberg & Levinson 2009)

PKS2155-304 (Aharonian et al. 2007)
See also Mrk501, PKS1222+21

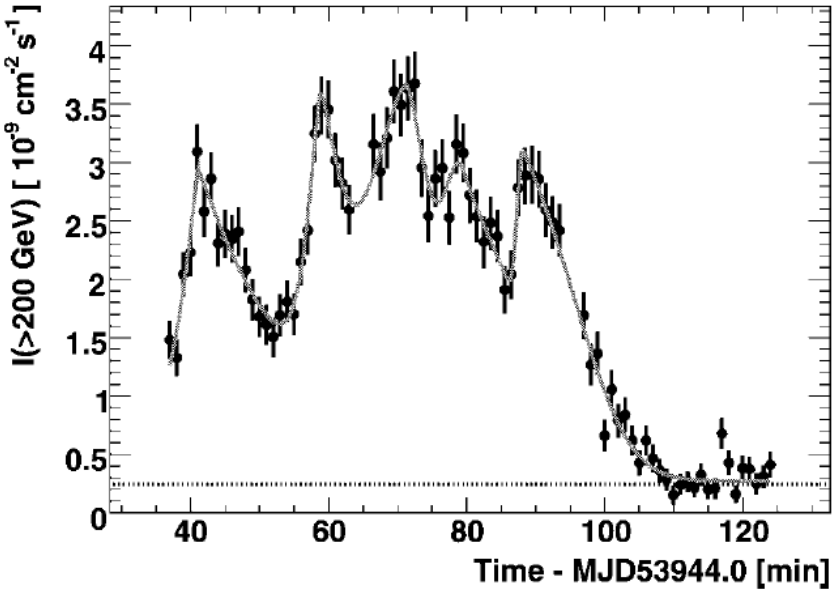

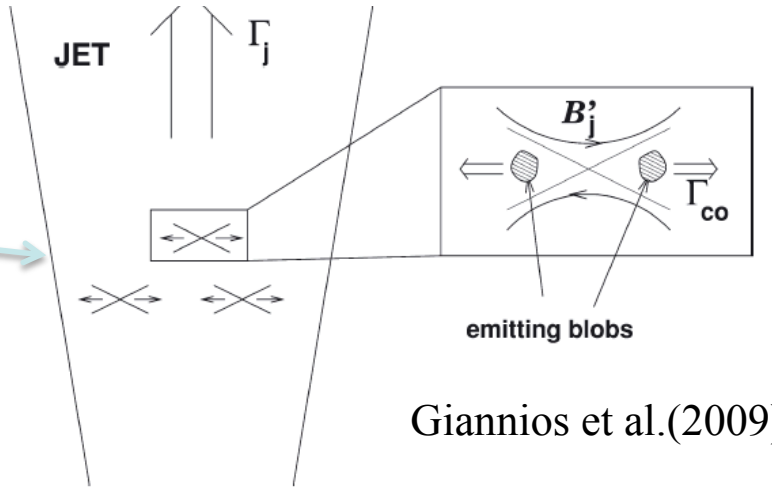

Giannios et al.(2009)

Jet Wobbling

- High resolution VLBI observations of some AGN jets show regular or irregular swings of innermost jet structural position angle (*jet wobbling*).
- Parsec scale AGN jet curvatures and helical-like structures (inner parsec or large scale) are believed to be triggered by changes in direction at the jet nozzle.
- Physical origin of jet wobbling (Agudo 2009)
  - Accretion disk precession
  - Orbital motion of accretion system (binary BH?)
  - Jet instabilities

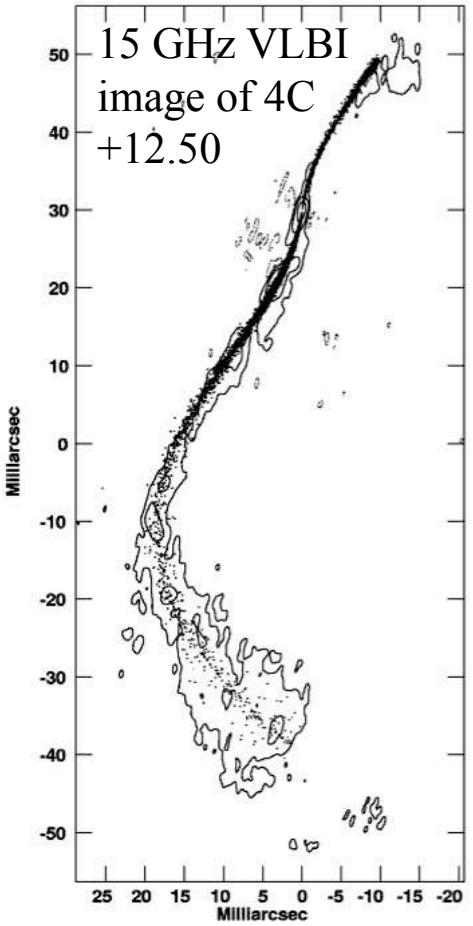

Position angle oscillation of 3C273

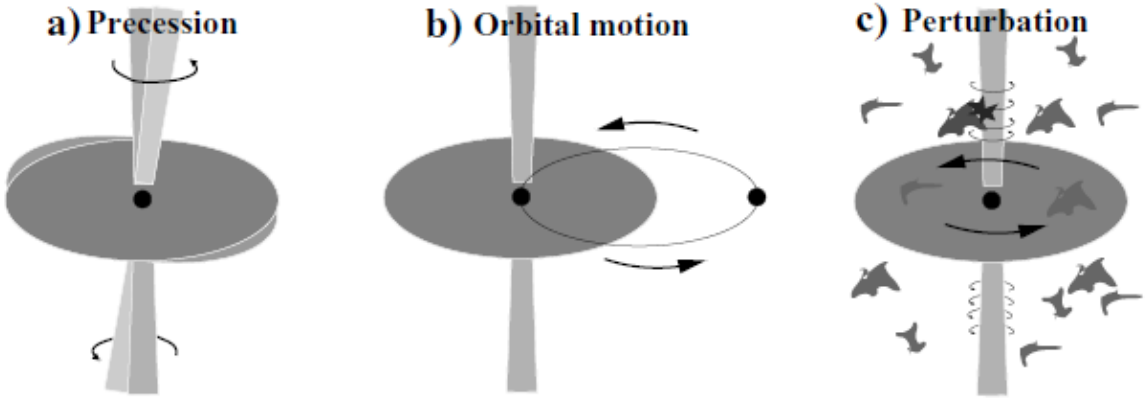

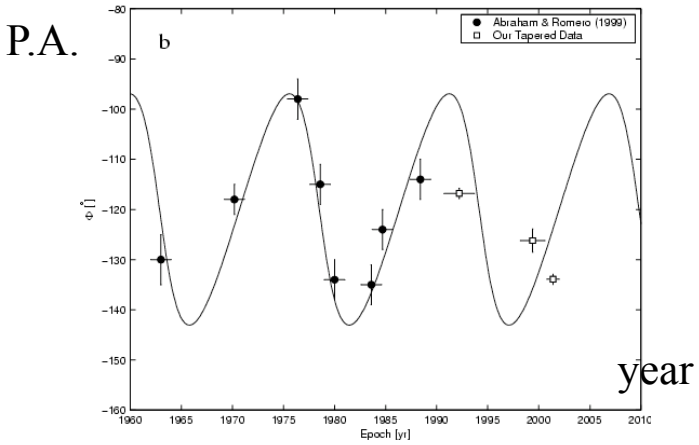

Instability of Relativistic Jets

•When jets propagate from magnetosphere of compact object (BH, NS), there are possibility to grow of two major instabilities

- Kelvin-Helmholtz (KH) instability
  - Important at the shearing boundary flowing jet and external medium
- Current-Driven (CD) instability
  - Important in existence of twisted magnetic field
  - Twisted magnetic field is expected jet formation simulation & MHD theory
  - Kink mode (*m=1*) is most dangerous in such system

- Instability of relativistic jet is important for understanding observed many jet phenomena & structure

  – quasi-periodic wiggles, knots, filaments, limb brightening, jet disruption etc

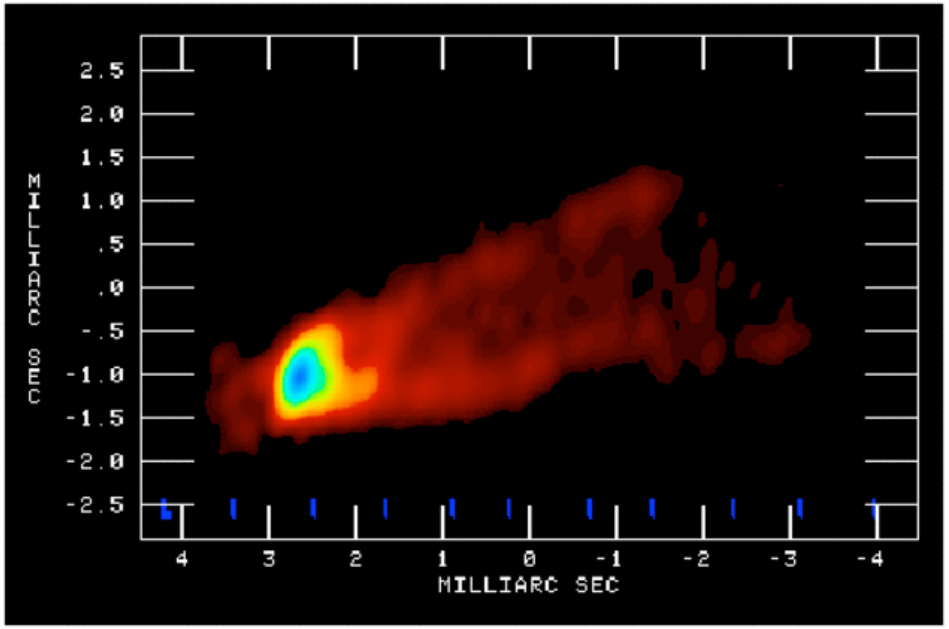

Limb brightening of M87 jets (observation)

Key Questions of Jet Stability

- When jets propagate outward, there are possibility to grow of two instabilities
  - Kelvin-Helmholtz (KH) instability
  - Current-Driven (CD) instability

- How do jets remain sufficiently stable?
- What are the Effects & Structure of KH / CD Instability in particular jet configuration (such as spine-sheath configuration)?

- We investigate these topics by using 3D relativistic MHD simulations

Regions of AGN Jet Propagation

Modified from Graphic courtesy David Meier

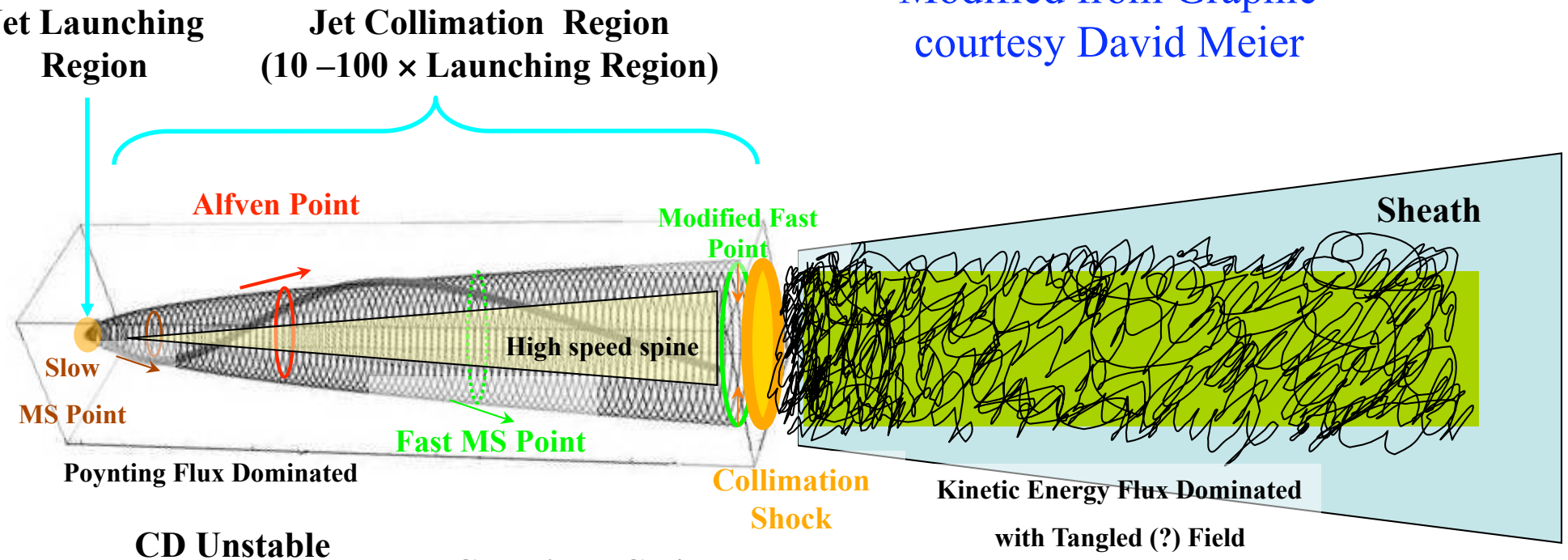

CD Kink Instability

- Well-known instability in laboratory plasma (TOKAMAK), astrophysical plasma (Sun, jet, pulsar etc).
- In configurations with strong toroidal magnetic fields, current-driven (CD) kink mode (m=1) is unstable.
- This instability excites large-scale helical motions that can be strongly distort or even disrupt the system
- For static cylindrical force-free equilibria, well known Kurskal-Shafranov (KS) criterion
  - Unstable wavelengths:

  $\lambda > |B_p/B_\phi| 2\pi R$
- However, rotation and shear motion could significant affect the instability criterion

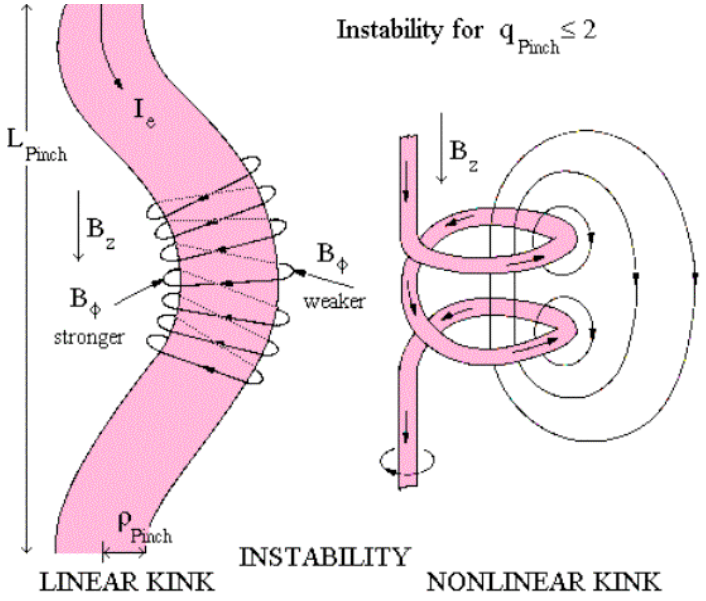

Schematic picture of CD kink instability

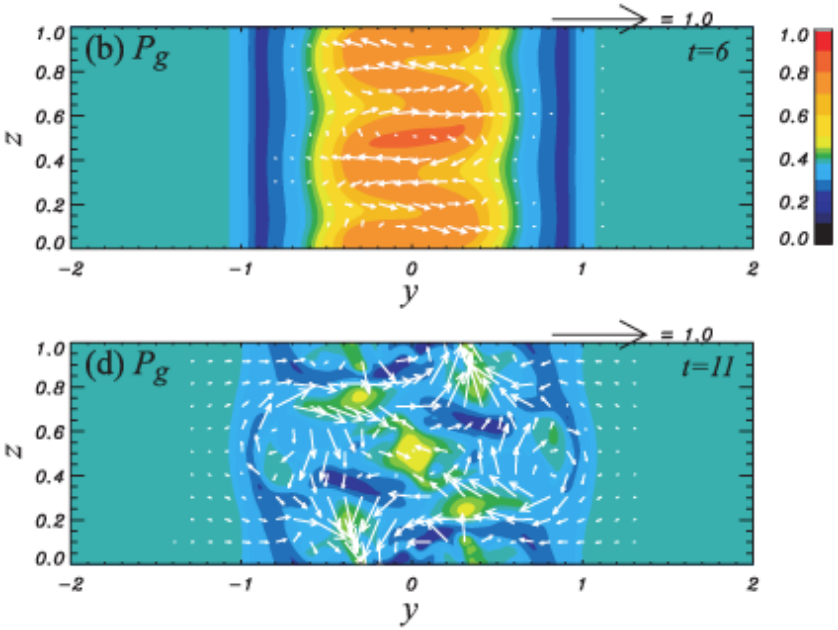

3D RMHD simulation of CD kink instability in PWNe (Mizuno et al. 2011)

CD Kink Instability in Jets (Newtonian)

Appl et al. (2000)

• Consider force-free field with different radial pitch profile in the rest frame of jet

• maximum growth rate: $\Gamma_{max}=0.133\ v_A/P_0$,

• unstable wave length: $\lambda_{max}=8.43P_0$

($P_0=a$ in our notation:
Magnetic pitch $=RB_z/B_\phi$)

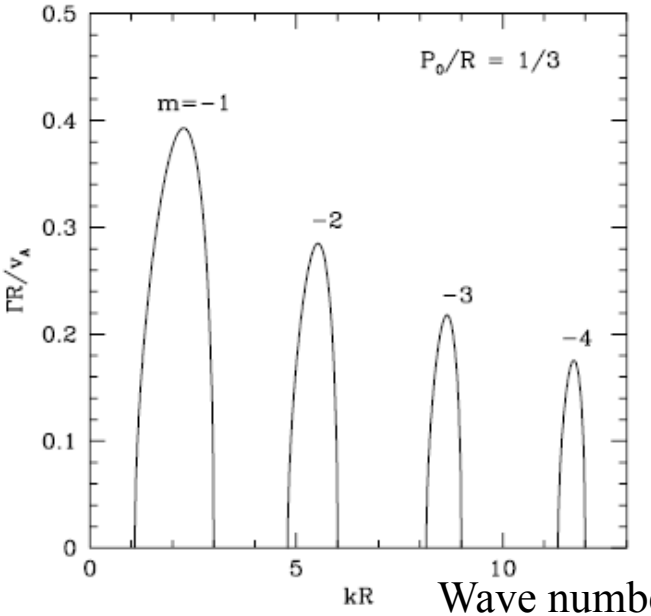

Wave number

Growth rate for m=-1~-4 in constant pitch case.

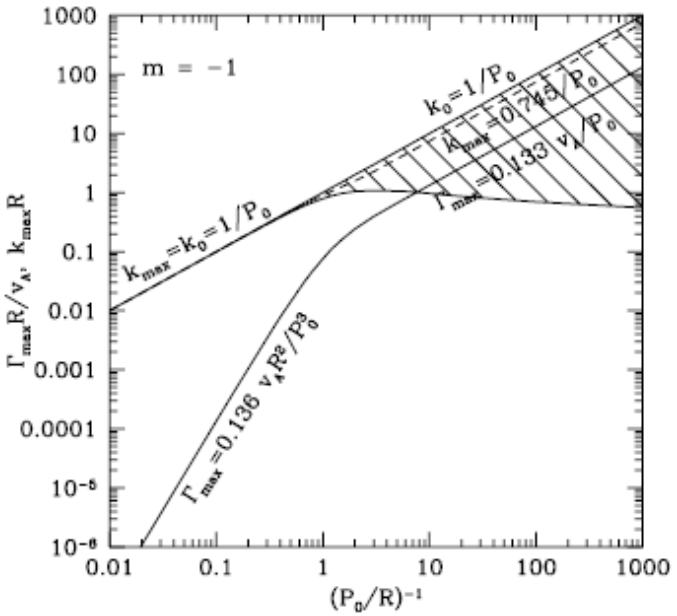

Maximum growth rate and unstable wave number for m=-1 kink as a function of magnetic Pitch

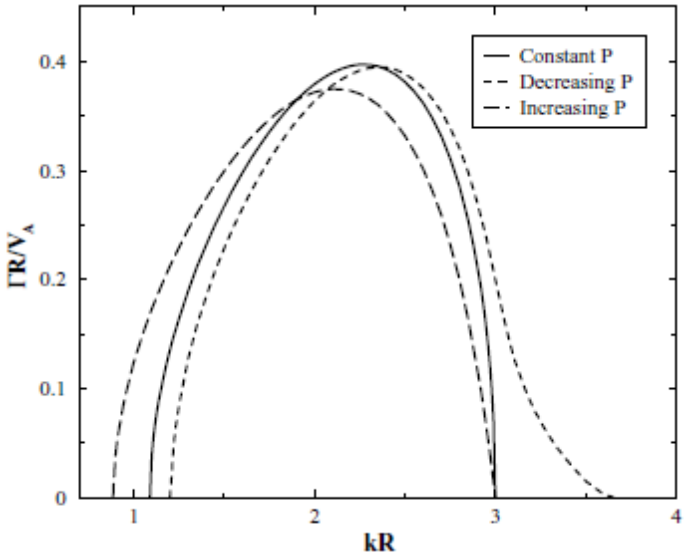

Growth rate for m=-1 mode as a function of wavenumber with different pitch profile

Previous Work for CD Kink Instability

- For relativistic force-free configuration
  - Linear mode analysis provides conditions for the instability but say little about the impact instability has on the system (Istomin & Pariev (1994, 1996), Begelman(1998), Lyubarskii(1999), Tomimatsu et al.(2001), Narayan et al. (2009))
  - Instability of potentially disruptive kink mode must be followed into the non-linear regime
- Helical structures have been found in Newtonian / relativistic simulations of magnetized jets formation and propagation (e.g., Nakamura & Meier 2004; Moll et al. 2008; McKinney & Blandford 2009; Mignone et al. 2010)

Purpose

- We investigate detail of non-linear behavior of relativistic CD kink instability
  - Relativistic: not only moving systems with relativistic speed but any with magnetic energy density comparable to or greater than the plasma energy density.
  - We start from static configurations because in the case of interest, the free energy is the magnetic energy, not kinetic energy
  - First task: static configuration (in generally, rigidly moving flows considered in the proper frame) are the simplest ones for studying the basic properties of the kink instability.

4D General Relativistic MHD Equation

- General relativistic equation of conservation laws and Maxwell equations:

$$\nabla_\nu (\rho U^\nu) = 0 \qquad \text{(conservation law of particle-number)}$$

$$\nabla_\nu T^{\mu\nu} = 0 \qquad \text{(conservation law of energy-momentum)}$$

$$\partial_\mu F_{\nu\lambda} + \partial_\nu F_{\lambda\mu} + \partial_\lambda F_{\mu\nu} = 0$$

$$\nabla_\mu F^{\mu\nu} = - J^\nu \qquad \text{(Maxwell equations)}$$

- Ideal MHD condition: $F_{\nu\mu} U^\nu = 0$
- metric : $ds^2 = -\alpha^2 dt^2 + g_{ij} (dx^i + \beta^i dt)(dx^j + \beta^j dt)$
- Equation of state : $p = (\Gamma - 1) u$

ρ : rest-mass density. p : proper gas pressure. u: internal energy. c: speed of light.
h : specific enthalpy, $h = 1 + u + p / \rho$.
Γ: specific heat ratio.
U^μ : velocity four vector. J^μ : current density four vector.
∇^μ : covariant derivative. $g_{\mu\nu}$: 4-metric. α : lapse function, β^i : shift vector, g_{ij} : 3-metric
$T^{\mu\nu}$: energy momentum tensor, $T^{\mu\nu} = p g^{\mu\nu} + \rho h U^\mu U^\nu + F^{\mu\sigma} F^\nu{}_\sigma - g_{\mu\nu} F^{\lambda\kappa} F_{\lambda\kappa} / 4$.
$F_{\mu\nu}$: field-strength tensor,

Conservative Form of GRMHD Equations (3+1 Form)

$$\frac{1}{\sqrt{-g}}\frac{\partial}{\partial t}(\sqrt{\gamma}D) + \frac{1}{\sqrt{-g}}\frac{\partial}{\partial x^i}(\sqrt{-g}D\tilde{v}^i) = 0,$$

(Particle number conservation)

$$\frac{1}{\sqrt{-g}}\frac{\partial}{\partial t}(\sqrt{\gamma}S_i) + \frac{1}{\sqrt{-g}}\frac{\partial}{\partial x^i}(\sqrt{-g}T^j_i) = T^{\mu\nu}\left(\frac{\partial g_{\nu i}}{\partial x^\mu} - \Gamma^\sigma_{\nu\mu}g_{\sigma i}\right)$$

(Momentum conservation)

$$\frac{1}{\sqrt{-g}}\frac{\partial}{\partial t}(\sqrt{\gamma}\tau) + \frac{1}{\sqrt{-g}}\frac{\partial}{\partial x^i}[\sqrt{-g}(\alpha T^{ti} - D\tilde{v}^i)] = \alpha\left(T^{\mu t}\frac{\partial \ln\alpha}{\partial x^\mu} - T^{\mu\nu}\Gamma^t_{\nu\mu}\right)$$

(Energy conservation)

$$\frac{1}{\sqrt{-g}}\frac{\partial}{\partial t}(\sqrt{\gamma}B^i) + \frac{1}{\sqrt{-g}}\frac{\partial}{\partial x^i}[\sqrt{-g}(\tilde{v}^jB^i - \tilde{v}^iB^j)] = 0.$$

(Induction equation)

U (conserved variables) F^i (numerical flux) S (source term)

$$D = \gamma\rho.$$

$$S_i = \alpha T^t_i = (\rho h + b^2)\gamma^2 v_j - \alpha b^0 b_j$$

$$\tau = \alpha^2 T^{tt} - D = (\rho h + b^2)\gamma^2 - (p + b^2/2) - \alpha^2(b^t)^2 - D.$$

$$\tilde{v}^i = v^i - \beta/\alpha$$

$\sqrt{-g}$: determinant of 4-metric
$\sqrt{\gamma}$: determinant of 3-metric

Detailed Features of the Numerical Schemes

Mizuno et al. 2006a, astro-ph/0609004 and progress

- RAISHIN utilizes conservative, high-resolution shock capturing schemes (Godunov-type scheme) to solve the 3D GRMHD equations *(metric is static)*

* *Reconstruction:* PLM (Minmod & MC slope-limiter function), convex ENO, PPM, WENO5, MP5, MPWENO5
* *Riemann solver:* HLL, HLLC, HLLD approximate Riemann solver
* *Constrained Transport:* Flux CT, Fixed Flux-CT, Upwind Flux-CT
* *Time evolution:* Multi-step Runge-Kutta method (2nd & 3rd-order)
* *Recovery step:* Koide 2 variable method, Noble 2 variable method, Mignore-McKinney 1 variable method
* *Equation of states:* constant Γ-law EoS, variable EoS for ideal gas

RAISHIN Code (3DGRMHD)

Mizuno et al. 2006a, 2011c, & progress

- RAISHIN utilizes conservative, high-resolution shock capturing schemes (Godunov-type scheme) to solve the 3D ideal GRMHD equations *(metric is static)*

Ability of RAISHIN code

- Multi-dimension (1D, 2D, 3D)
- Special & General relativity (static metric)
- Different coordinates (RMHD: Cartesian, Cylindrical, Spherical and GRMHD: Boyer-Lindquist of non-rotating or rotating BH)
- Different schemes of numerical accuracy for numerical model (spatial reconstruction, approximate Riemann solver, constrained transport schemes, time advance, & inversion)
- Using constant Γ-law and general Equation of State (Synge-type)
- Parallel computing (based on OpenMP, MPI)

Ability of RAISHIN code

- Multi-dimension (1D, 2D, 3D)
- Special and General relativity (static metric)
- Different coordinates (RMHD: Cartesian, Cylindrical, Spherical and GRMHD: Boyer-Lindquist of non-rotating or rotating BH)
- Different spatial reconstruction algorithms (7)
- Different approximate Riemann solver (4)
- Different constrained transport schemes (3) or divergence cleaning schemes (1)
- Different time advance algorithms (2)
- Different recovery schemes (3)
- Using constant Γ-law and variable Equation of State (Synge-type)
- Parallelized by OpenMP, MPI

Initial Condition for Static Plasma Column

Mizuno et al. (2009)

- Solving ideal RMHD equations using RAISHIN in Cartesian coordinates
- Static Cylindrical Plasma column with force-free equilibrium helical magnetic field
- Magnetic pitch ($P=RB_z/B_\phi$): constant, increase, decrease
- Density profile: constant or decrease ($\rho=\rho_0 B^2$)
- Numerical box: $-2L < x, y < 2L$, $0 < z < 2L$ (Cartesian coordinates:160 x 160 x 80 zones)
- Boundary: periodic in axial (z) direction
- Small velocity perturbation with $m=1(-1)$ and $n=1(-1)$ modes

$$v_R = \delta v \exp\left(-\frac{R}{R_a}\right)\cos(m\theta)\sin\left(\frac{2\pi n z}{L_z}\right)$$

Force-Free Helical Magnetic Field

Force-free equilibrium: $$B_z \frac{dB_z}{dR} + \frac{B_\phi}{R}\frac{dB_\phi}{dR} = 0.$$

Measured in Laboratory frame

Choose poloidal magnetic field: $$B_z = \frac{B_0}{[1+(R/a)^2]^\alpha},$$

B_0: magnetic amplitude
a: characteristic radius
$a=1/8L$ in this work
α: pitch profile parameter

Find toroidal magnetic field:

$$B_\phi = \frac{B_0}{(R/a)[1+(R/a)^2]^\alpha}\sqrt{\frac{[1+(R/a)^2]^{2\alpha}-1-2\alpha(R/a)^2}{2\alpha-1}}$$

Magnetic pitch ($P = RB_z/B_\phi$) :

$$P = (R/a)^2\sqrt{\frac{2\alpha-1}{[1+(R/a)^2]^{2\alpha}-1-2\alpha(R/a)^2}}$$

$\alpha < 1$ ⇒ pitch increase

$\alpha=1$ ⇒ constant helical pitch (same as previous non-relativistic work)

$\alpha > 1$ ⇒ helical pitch decrease

Initial Radial Profile

Magnetic pitch

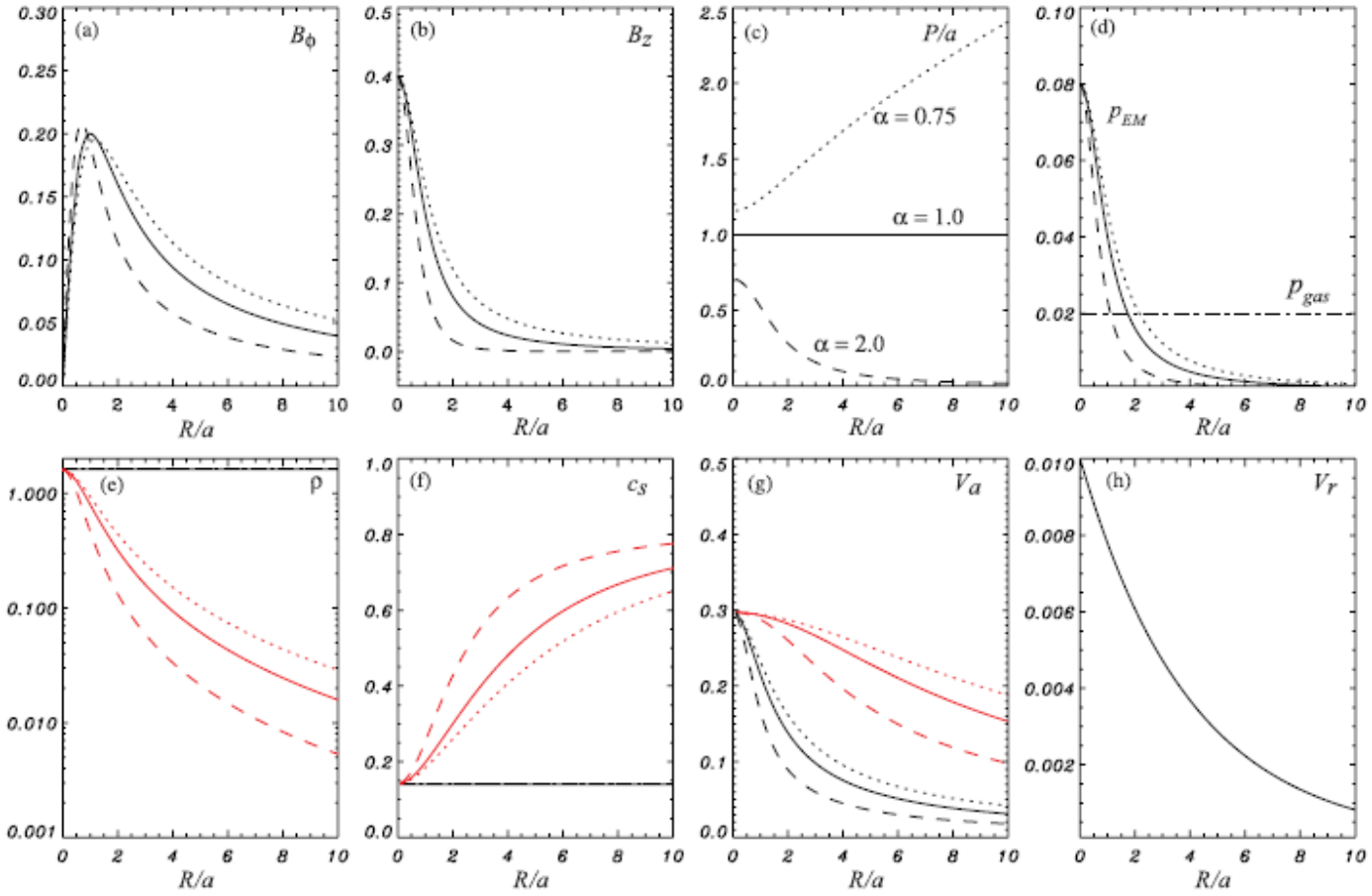

density Sound velocity Alfven velocity

Black: constant density
Red: decreasing density

Solid: constant pitch
dotted: increase pitch
Dashed: decrease pitch

3D Structure
(Decrease density with Constant pitch)

- Displacement of the initial force-free helical magnetic field leads to a helically twisted magnetic filament around the density isosurface by CD kink instability
- Slowly continuing outwards radial motion is confined to a lower density sheath around the high density core

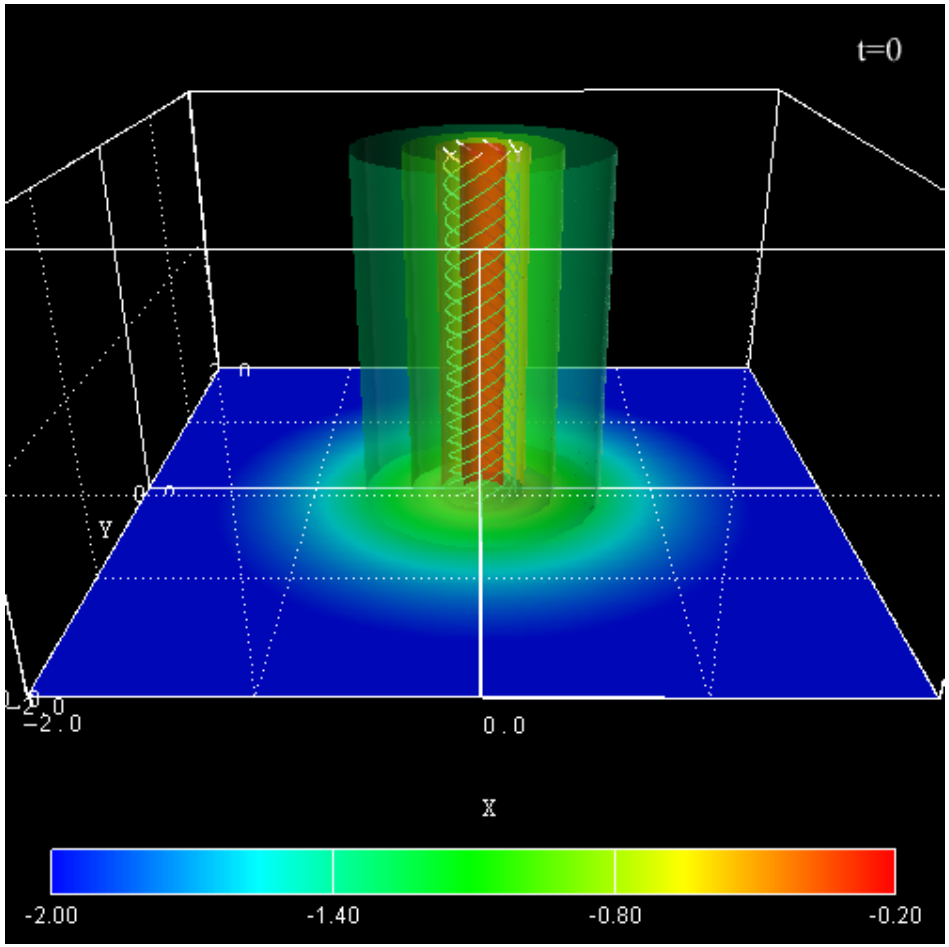

Color: density
White line: magnetic field lines

Dependence on pitch profile

t_A: Alfven crossing time

Increase pitch

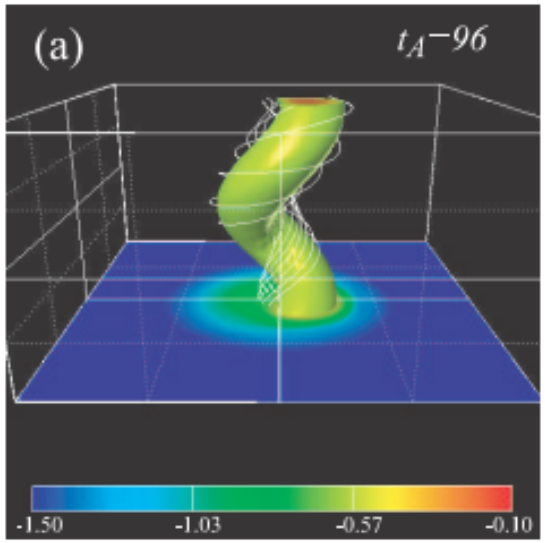

Constant pitch

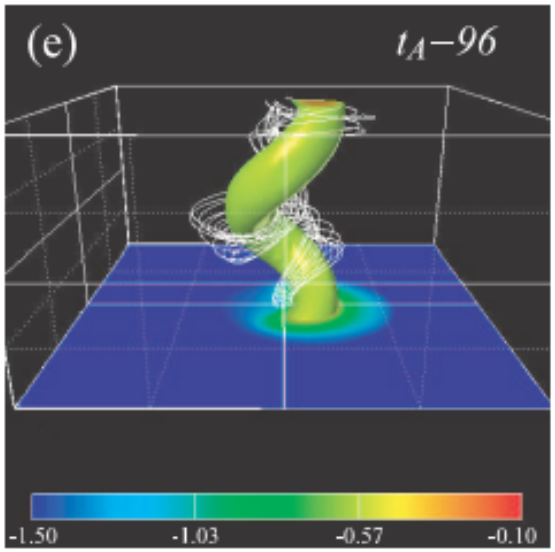

Decrease pitch

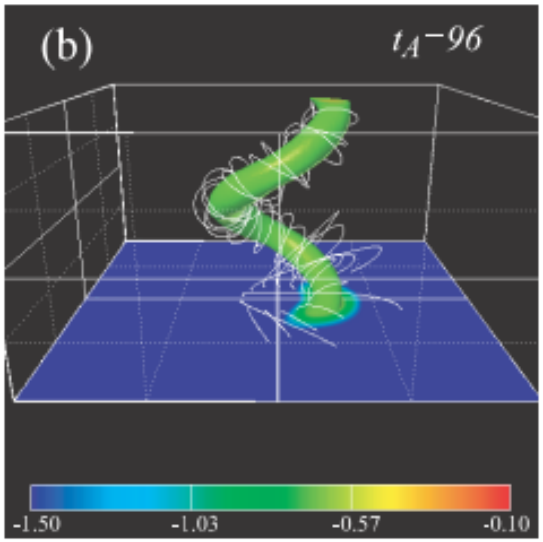

Constant pitch: Amplitude growth slows at later time.

Increase pitch: 3D density structure looks similar to constant pitch case.
However, amplitude growth ceases at later time.

Decrease pitch: slender helical density wrapped by B-field developed.
Amplitude growth continues throughout simulation.

Time evolution

Volume-averaged kinetic energy transverse to the z-axis

Constant density

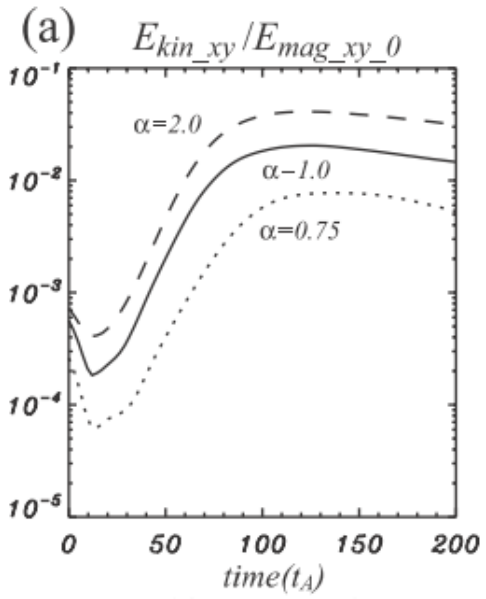

Decrease density

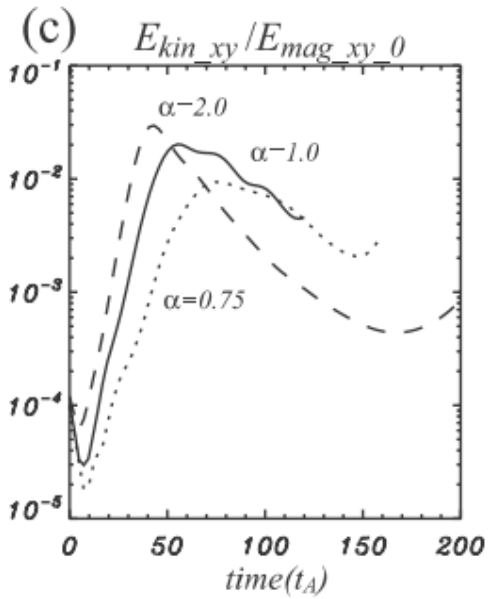

t_A: Alfven crossing time

Solid: constant pitch
Dotted: increase pitch
Dashed: decrease pitch

- Initial exponential linear growth phase and subsequent non-linear evolution
- Density Decline: more rapid initial growth and decline (by more gradual radial decline in the Alfven velocity) .
- Pitch increase: slower growth
- Pitch decrease: more rapid growth

- Consistent with non relativistic linear analysis in Appl et al. (2000)

CD kink instability of Sub-Alfvenic Jets: Temporal Properties

- At the next stage, we investigate the influence of jet shear motions on the stability and nonlinear behavior of CD kink instability.
- We consider sub-Alfvenic jets because this configuration is stable against KH instability.
- Only focus on CD kink instability at this work.

Initial Condition for Sub-Alfvenic top-hat Jets Mizuno et al. (2011)

- Cylindrical sub-Alfvenic jets ($v_j=0.2c$) with force-free helical magnetic field (stable against KH instability)
- Magnetic pitch ($P=RB_z/B_\phi$): constant, increase, decrease
- Density profile: decrease ($\rho=\rho_0 B^2$)
- Jet radius: $R_j=1/2a,\ a,\ 2a,\ 4a$
- Numerical box: $-2L < x, y < 2L,\ 0 < z < 3L$ (Cartesian coordinates:160 x 160 x 120 zones)
- Boundary: periodic in axial (z) direction
- Small radial velocity perturbation with $m=1(-1)$ and $n=1(-1)$ modes

$$v_R = \delta v \exp\left(-\frac{R}{R_a}\right)\cos(m\theta)\sin\left(\frac{2\pi n z}{L_z}\right)$$

Initial Force-Free Configuration

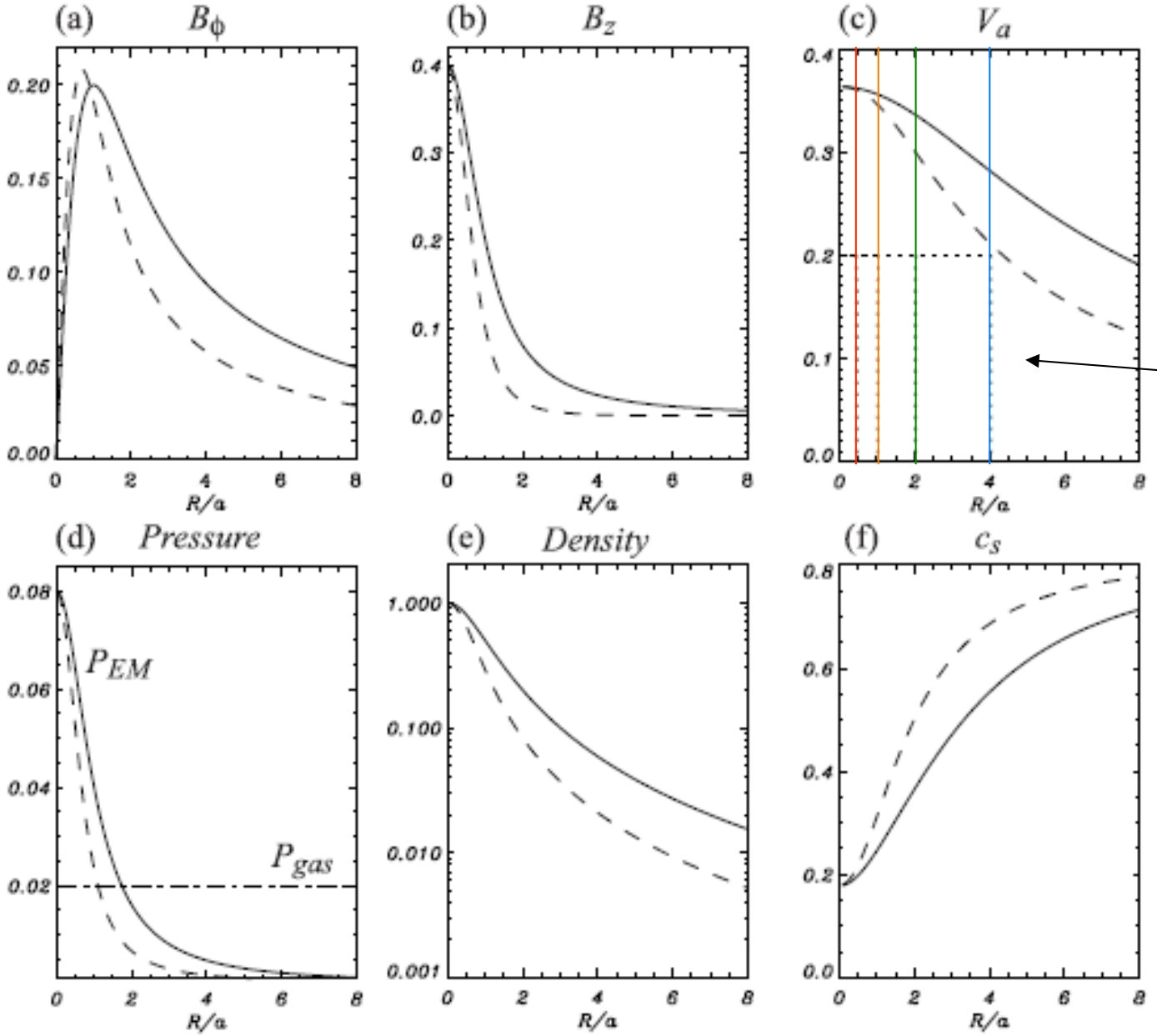

Solid: constant pitch
Dashed: decrease pitch

Jet position

Time evolution of 3D structure

•V_j=0.2c, R_j=2a, constant pitch

•Similar to static case, displacement of the initial force-free helical field leads to a helically twisted magnetic filament around the density isosurface by CD kink instability

•From transition to non-linear stage, helical twisted structure is propagates along jet axis with continuous increase of kink amplitude.

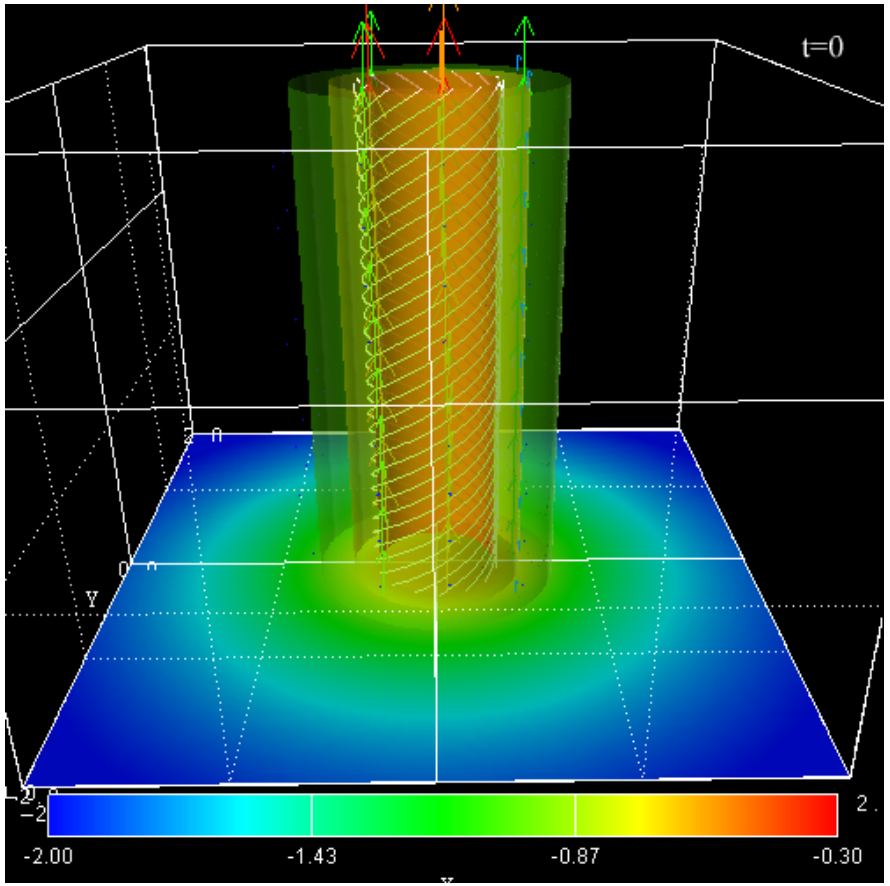

Color: density
White line: magnetic field lines
Vectors: velocity

Dependence on Jet Radius

Volume-averaged kinetic and magnetic energies

Red: $R_j=1/2a$, Orange: $R_j=a$, Green: $R_j=2a$,
Blue: $R_j=4a$, Black: no jet

- Initial exponential linear growth phase and subsequent non-linear evolution similar to static (no jet) case

- Larger jet radius: slower linear growth with larger maximum amplitude by jet shear effect
- Far from characteristic radius, $R_j >> a$: jet shear effect becomes weaker and approached to static case
(static case = rigidly moving flow seen in jet frame)

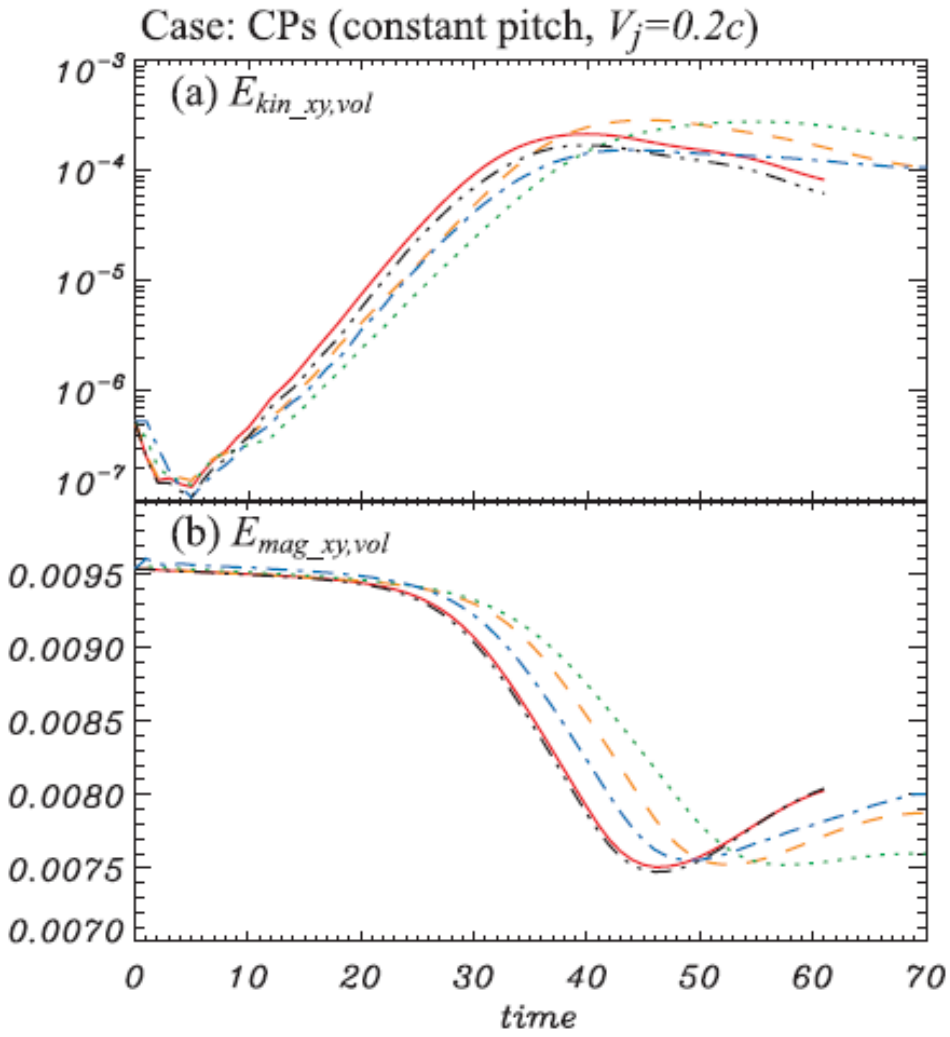

Dependence on Jet Radius

3D helical structure

- No difference in helical kink structure

- $R_j \sim a$: flow follows helical kink structure
- $R_j > a$: keep initial straight jet flow even in nonlinear stage (= rigidly moving flow)

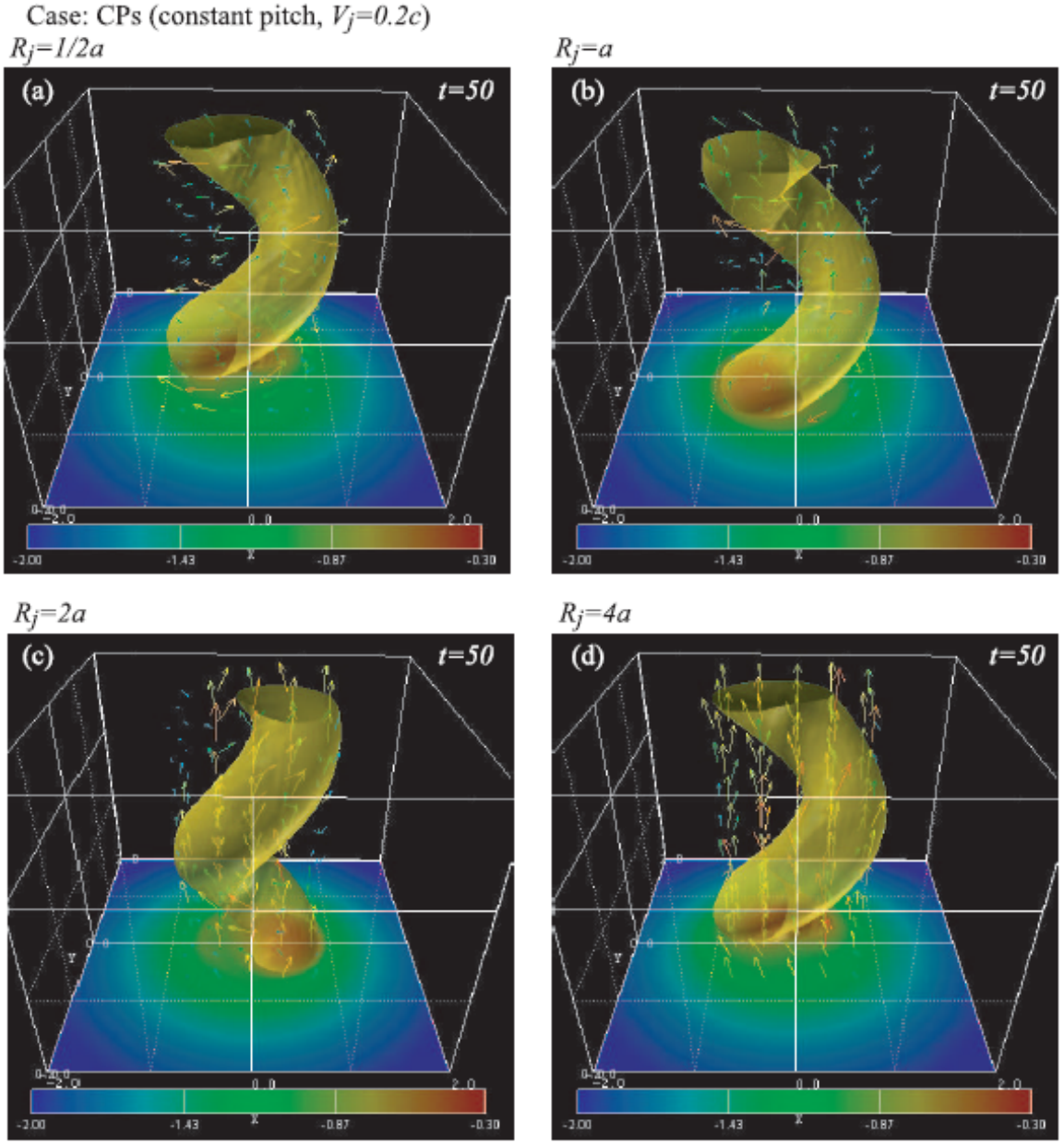

Propagation of Helical Structure

Maximum density position at z=8a

Red: $R_j=1/2a$, Orange: $R_j=a$, Green: $R_j=2a$, Blue: $R_j=4a$, Black: no jet

Rj=2a case

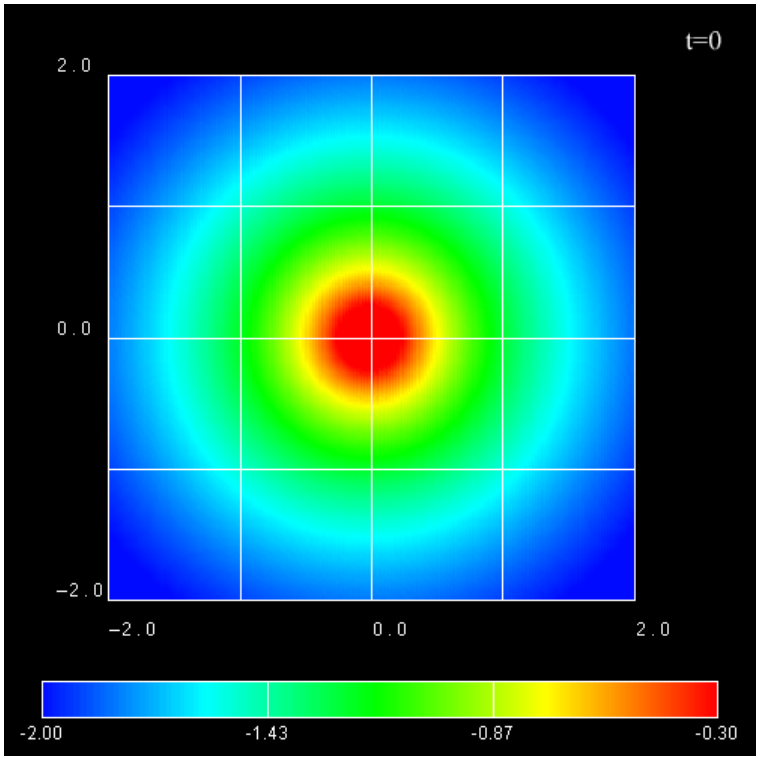

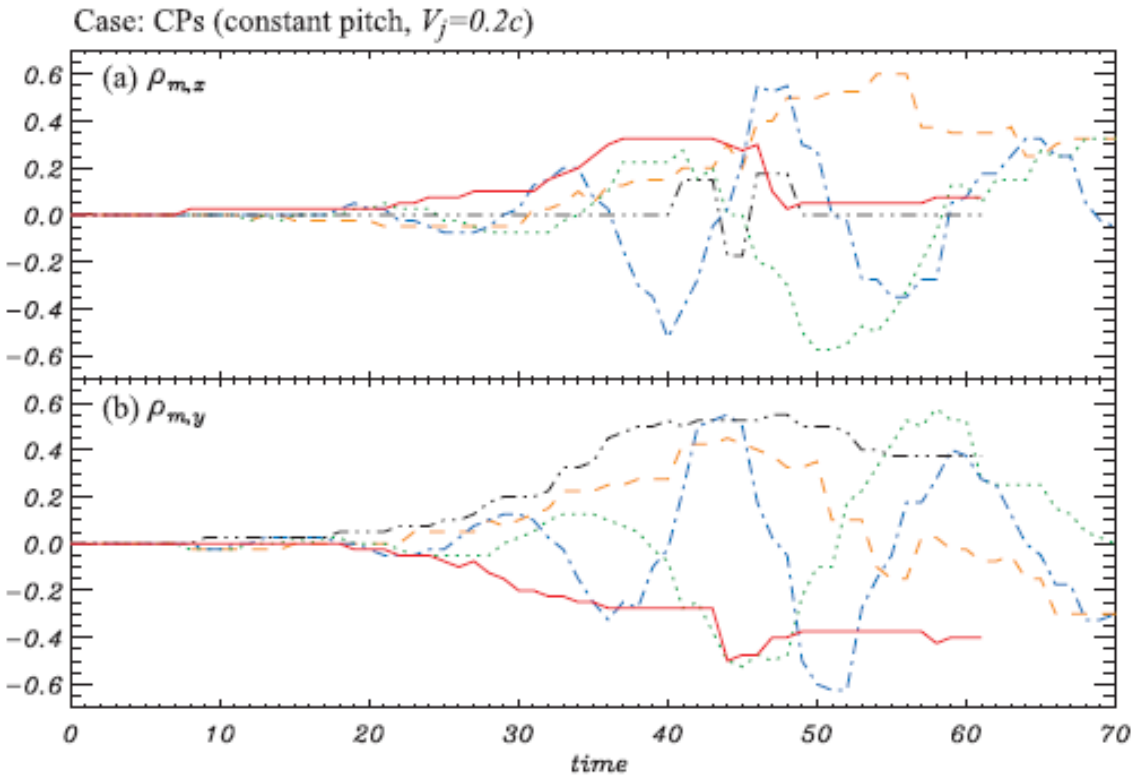

- $R_j > a$: clearly shown the propagation of helical structure along jet.
- larger jet radius: faster propagation speed ($\sim V_j$) .
- Propagation speed is decreasing with time.

CD kink instability of Rotating Relativistic Jets: Temporal Properties

- At the next step, we investigate the influence of jet rotation on the stability and nonlinear behavior of CD kink instability.
- We consider differentially rotating relativistic jets motivated from analysis of the structure of Poynting-flux dominated jets (Lyubarsky 2009).
- In cylindrically equilibrium configurations (close to force-free), the poloidal and toroidal fields are comparable in the comoving frame.
- The jet structure relaxes to a locally equilibrium configuration if the jet is narrow enough (the Alfven crossing time is less than the proper propagation time).

Initial Condition for Rotating Relativistic Jets

Mizuno et al. (2012)

- Differential rotation relativistic jet with force-free helical magnetic field
- Magnetic pitch ($P=RB_z/B_\phi$): constant
- Angular velocity (Omega_0=0,1,2,4,6)
- Density profile: decrease ($\rho=\rho_0 B^2$)
- Numerical box: $-3L < x, y < 3L$, $0 < z < 3L$ (Cartesian coordinates: 240 x 240 x 120 zones)
- Boundary: periodic in axial (z) direction
- Small velocity perturbation with $m=1$ and $n=0.5 \sim 4$ modes

$$v_R/c = \frac{\delta v}{N} \exp\left(-\frac{R}{R_p}\right) \sum_{n=1}^{N} \cos(m\theta) \sin\left(\frac{\pi n z}{L_z}\right)$$

Force-Free Helical Magnetic Field and Velocity

Force-free equilibrium: $\frac{\Omega B_z}{c^2}\frac{d}{dR}\Omega R^2 B_z = B_z\frac{dB_z}{dR} + \frac{B_\phi}{R}\frac{dB_\phi}{dR}$

Measured in comoving frame

Choose poloidal magnetic field: $B_z = \frac{B_0}{[1+(R/R_0)^2]^\alpha}$

Choose Angular velocity: $\Omega = \begin{cases} \Omega_0 & \text{if } R \le R_0 \\ \Omega_0 (R_0/R)^\beta & \text{if } R > R_0 \end{cases}$

B_0: magnetic amplitude
R_0: characteristic radius
R_0=*1/4L* in this work
α: pitch profile parameter
β: differential rotation parameter
α=*1*, β=*1* in this work

Find toroidal magnetic field:

$$B_\phi = -\frac{B_0}{R[1+(R/R_0)^2]^\alpha}\sqrt{\frac{\Omega^2 R^4}{c^2} + \frac{R_0^2[1+(R/R_0)^2]^{2\alpha} - R_0^2 - 2\alpha R^2}{2\alpha - 1}}$$

Magnetic pitch ($P = RB_z/B_\phi$) :

$$P = R^2\sqrt{\frac{2\alpha-1}{(2\alpha-1)(\Omega R^2/c)^2 + R_0^2[1+(R/R_0)^2]^{2\alpha} - R_0^2 - 2\alpha R^2}}$$

Jet Velocity (Drift velocity):

$$v_z = -\frac{B_\phi B_z}{B^2}\Omega R,$$

$$v_\phi = (1 - \frac{B_\phi^2}{B^2})\Omega R.$$

Initial Radial Profile

solid: Ω_0=0
dotted: Ω_0=1
dashed: Ω_0=2
dash-dotted: Ω_0=4
dash-two-dotted: Ω_0=6

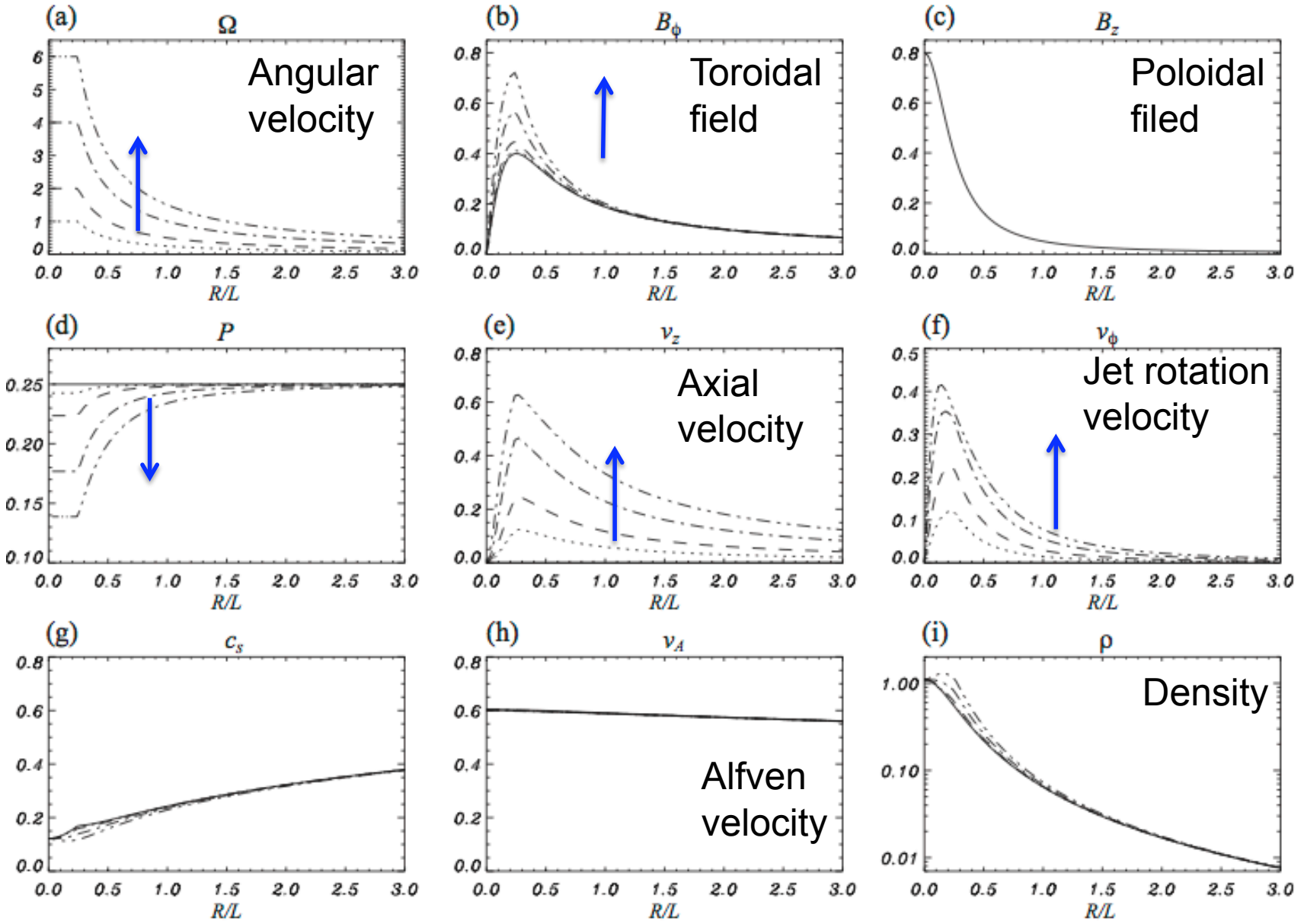

Time Evolution of 3D Structure

- Similar to static case, displacement of the initial force-free helical field leads to a helically twisted magnetic filament around the density isosurface with n=1 mode by CD kink instability
- From transition to non-linear stage, helical twisted structure is propagates in flow direction with continuous increase of kink amplitude.
- The propagation speed of kink ~0.1c (similar to initial maximum axial drift velocity)

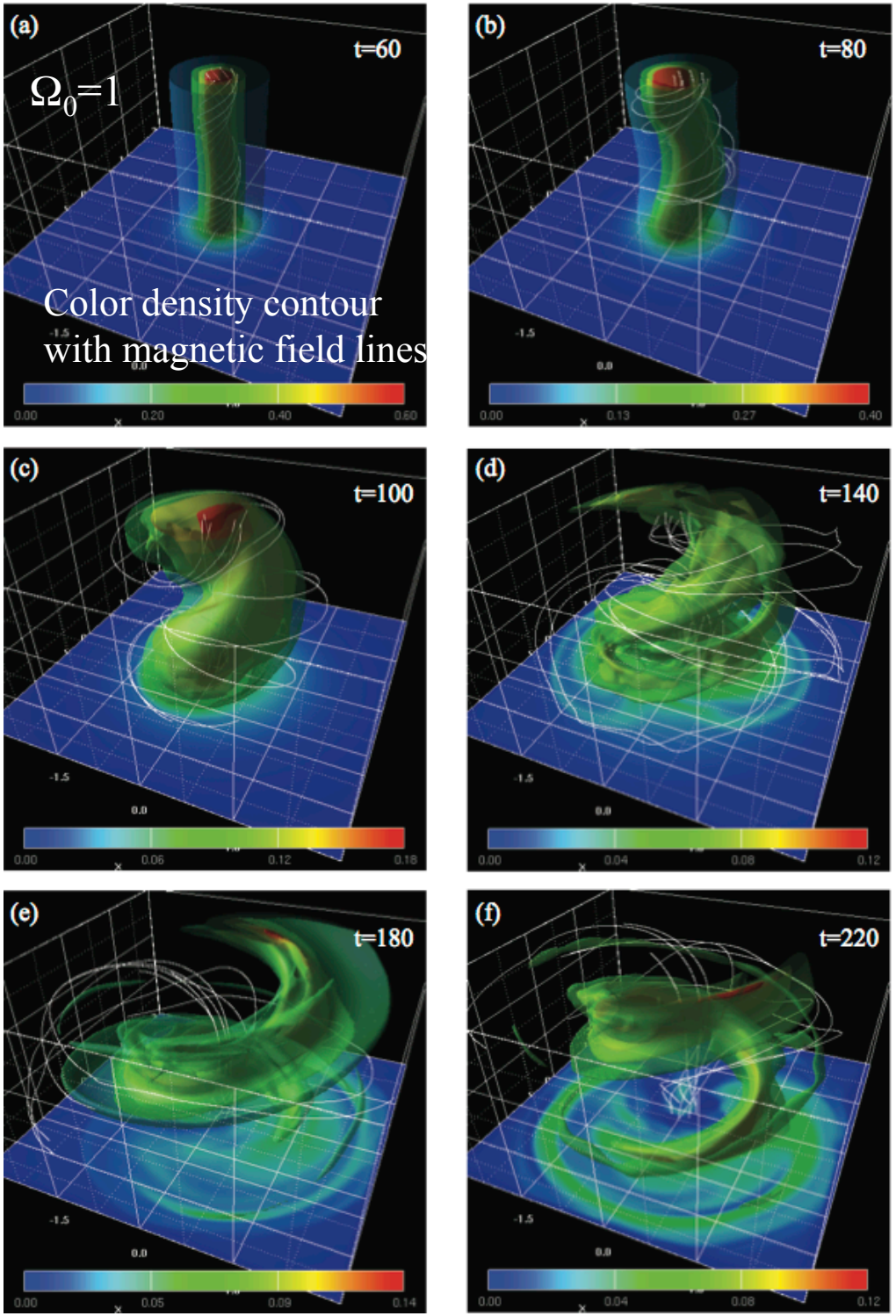

Dependence on Jet Rotation Velocity: growth rate

solid: Ω_0=0
dotted: Ω_0=1
dashed: Ω_0=2
dash-dotted: Ω_0=4
dash-two-dotted: Ω_0=6

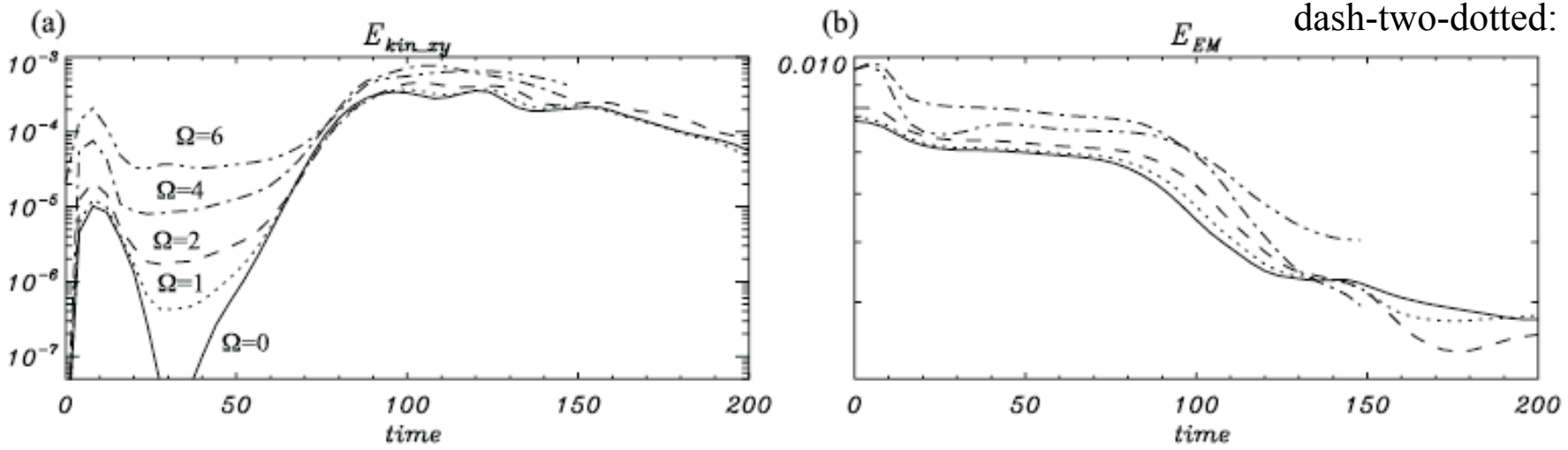

- First bump at t < 20 in E_{kin} is initial relaxation of system
- Initial exponential linear growth phase from t ~ 40 to t ~120 (dozen of Alfven crossing time) in all cases
- Agree with general estimate of growth rate, $\Gamma_{max} \sim 0.1 v_A/R_0$

- Growth rate of kink instability does not depend on jet rotation velocity

Dependence on Jet Rotation Velocity: 3D Structure

- Ω_0=2 case: very similar to Ω_0=1 case, excited n=1 mode
- Ω_0=4 & 6 cases: n=1 and n=2 modes start to grow near the axis region
- It is because pitch decrease with increasing Ω_0
- In nonlinear phase, n=1 mode wavelength only excited in far from the axis where pitch is larger
- Propagation speed of kink is increase with increase of angular velocity

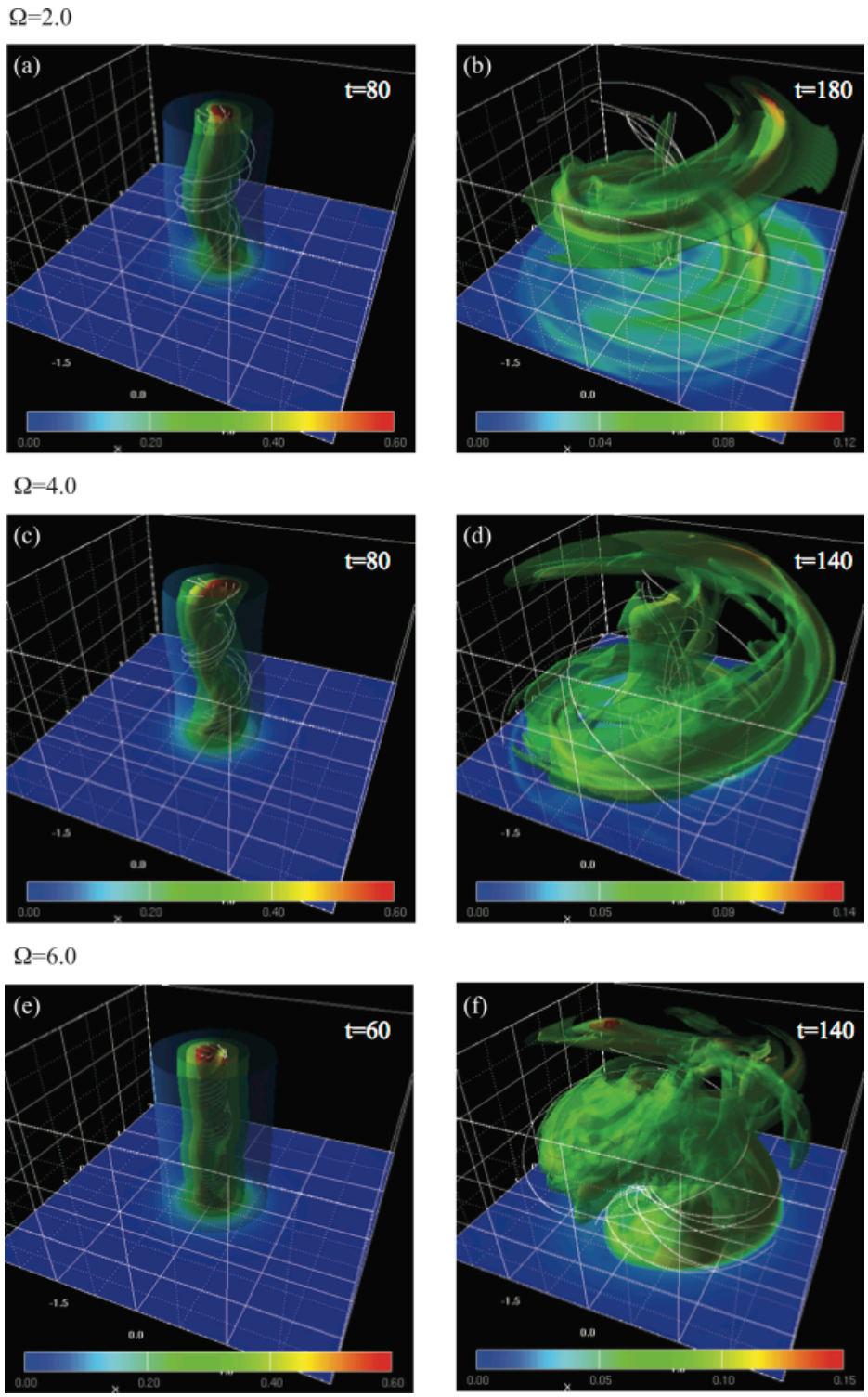

Multiple Mode Interaction

- In order to investigate the multiple mode interaction, perform longer simulation box cases with Ω_0=2 & 4
- Ω_0=2 case: n=1 and n=2 modes grow near the axis region (n=1 mode only in shorter box case)
- In nonlinear phase, growth of the CD kink instability produces a complicated radially expanding structure as a result of the coupling of multiple wavelengths
- Cylindrical jet structure is almost disrupted in long-term evolution.
- The coupling of multiple unstable wavelengths is crucial to determining whether the jet is eventually disrupted.

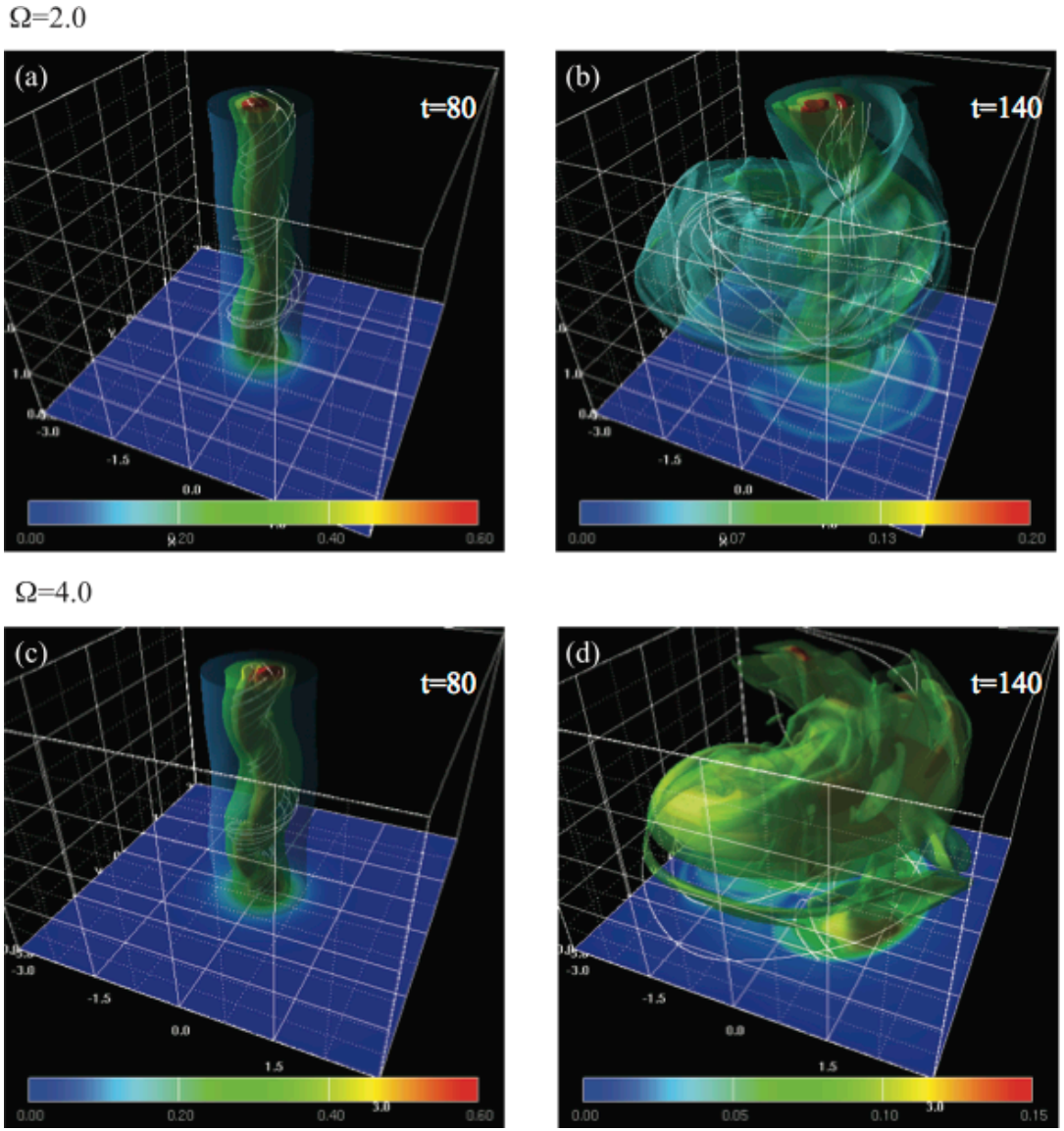

CD kink instability of Sub-Alfvenic Jets: Spatial Properties Mizuno et al. 2013, in prep

Initial Condition

- Cylindrical sub-Alfvenic (top-hat) non-rotating jet established across the computational domain with a helical force-free magnetic field
  - V_j=0.2c, R_j=1.0
- Radial profile: Decreasing density with constant magnetic pitch ($a=1/4L$)
- Jet spine precessed to break the symmetry ($\lambda\sim 3L$)

Preliminary Result

- Precession perturbation from jet inlet produces the growth of CD kink instability with helical density distortion.
- Helical structure propagates along the jet with continuous growth of kink amplitude in non-linear phase.

3D density with magnetic field lines $t=L/c$

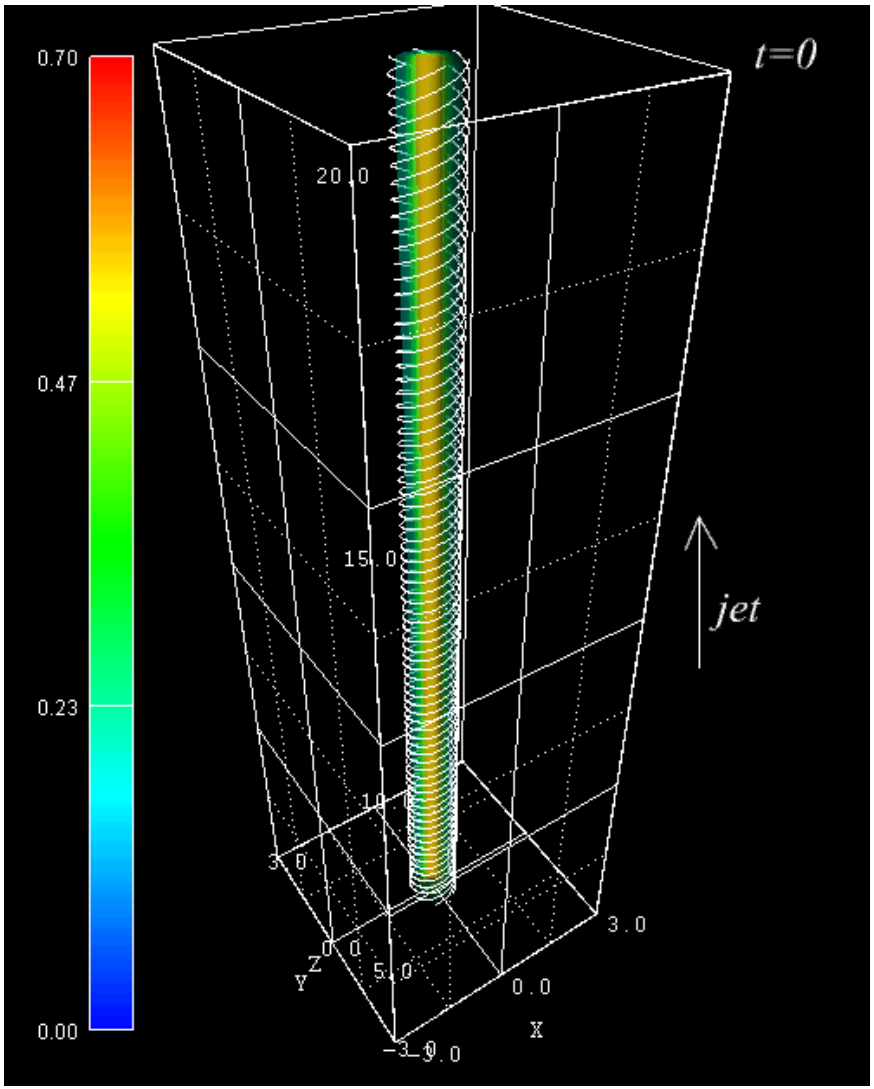

Summery

- In CD kink instability of static plasma column, we found the initial configuration is strongly distorted but not disrupted.
- The linear growth and nonlinear evolution of the CD kink instability depends on the radial density profile and strongly depends on the magnetic pitch profile
- In rotating relativistic jet case, developed helical kink structure propagates along jet axis with continuous growth of kink amplitude.
- The coupling of multiple unstable wavelengths is crucial to determining whether the jet is eventually disrupted in nonlinear stage.
- The strongly deformed magnetic field via CD kink instability may trigger of magnetic reconnection in the jet (need RRMHD simulation).

Relativistic Magnetic Reconnection using RRMHD Code

Mizuno 2013, ApJS, in press

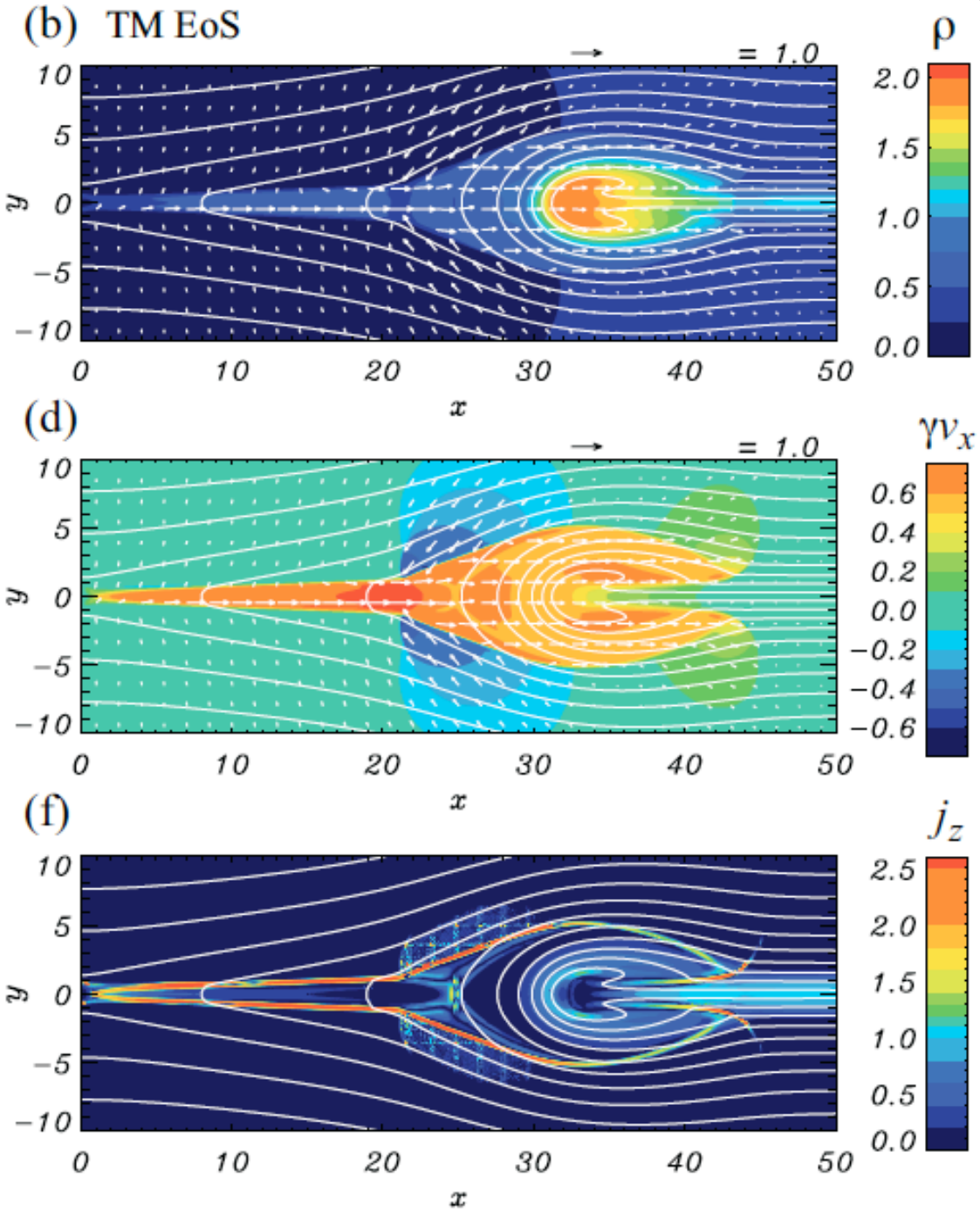

Assumption

• Consider Pestchek-type magnetic reconnection

Initial condition

• Harris-type model（anti-parallel magnetic field）

• Anomalous resistivity for triggering magnetic reconnection （r<0.8）

Results

• B-filed：typical X-type topology

• Density：Plasmoid

• Reconnection outflow: ~0.8c

Future works

- Effect of jet rotation for development of CD kink instabilities
- Coupling of CD kink/KH instabilities of super-Alfvenic jets
  - Temporal and spatial properties
- Relativistic magnetic reconnection
  - Development of resistive relativistic MHD code
- Effect of perturbation for Relativistic jet formation
  - Relation between disk perturbation and formed jet structure
- Radiation image/polarization from relativistic jet formation and propagation

Other Research

- General relativistic MHD simulations of collapsar as the central engine of GRBs (Mizuno et al. 2004ab)
- Development of 3D general relativistic MHD code RAISHIN (Mizuno et al. 2006a, 2011c)
- General relativistic MHD simulations of relativistic jet formation from thin Keplerian disk (Mizuno et al. 2006b, Hardee et al. 2007)
- Radiation imaging from BH-accretion disk system (Wu et al. 2008)
- MHD effect for relativistic shock and additional jet acceleration (Mizuno et al. 2008, 2009)
- Magnetic Field Amplification by relativistic turbulence in propagating relativistic shock (Mizuno et al. 2011a)
- Relaxation of Pulsar wind nebulae via CD kink instability (Mizuno et al. 2011b)
- Relativistic Particle-in-Cell simulations of relativistic jets (Nishikawa et al. 2009)

M87 Jet & BH

Basic facts: D ~ 16.7 Mpc , 1” ~ 80 pc

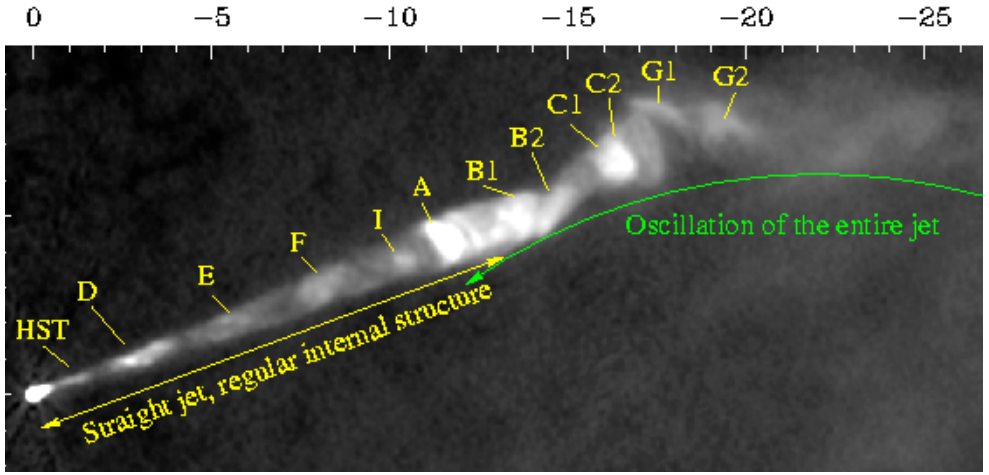

Nuclear region: M_{bh} ~ 6 x 10^9 M_{sol} , R_s ~ 0.6 ***milli***-pc

Gebhardt & Thomas (2009)

Junor, Biretta & Livio (1999)

Ly, Walker & Wrobel (2004)

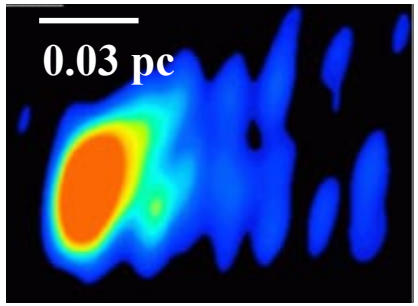

Biretta, Junor & Livio (2002)

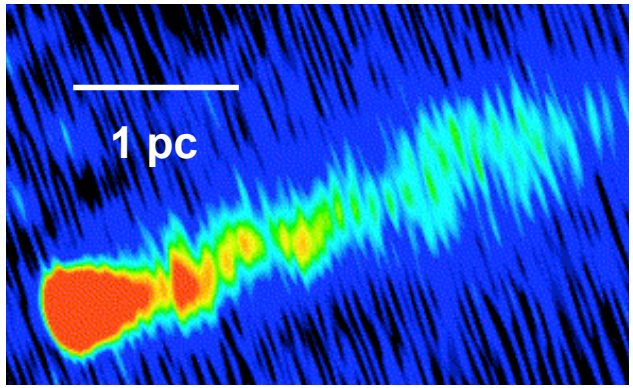

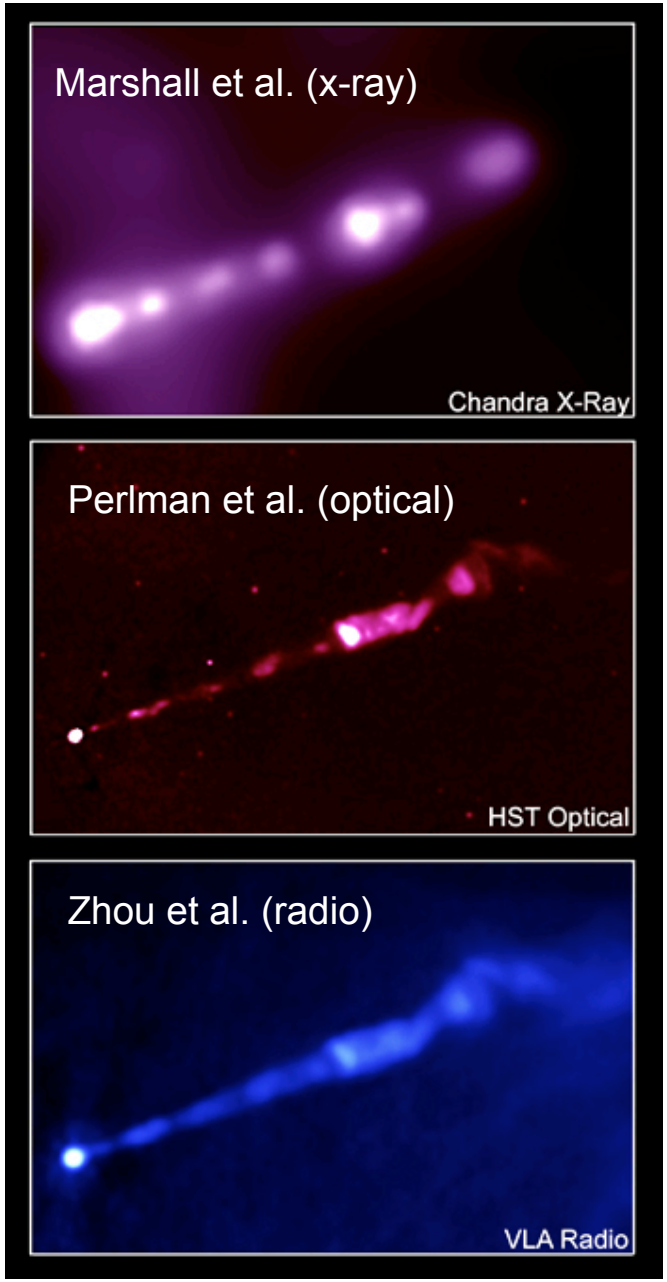

M87: BH & Jet Collimation Region

Radio Galaxy	FR Type	M_{BH} ($M_\odot$)	D (pc)	R_S/μas	Collimation Region Size
M87/Vir A	I	6.0×10^9	1.67×10^7	7.5	0.10 – 10 mas
Cen A	I	2.0×10^8	3.4×10^6	1.2	0.06 – 6 mas
Cyg A	II	2.5×10^9	2.2×10^8	0.2	2.2 – 44 μas
Sgr A	GC	2.5×10^6	8,500	5.9	0.07 – 7 mas

M87 Black Hole & Jet Launching Region Largest Angular Size!

3D RHD Jet Simulations & Linear Analysis

RHD Jet Dispersion Relation Solutions (Linear analysis)

v_w=0.0 Helical Mode (v_w = 0) Helical Mode (v_w = 0.5) v_w=0.5c

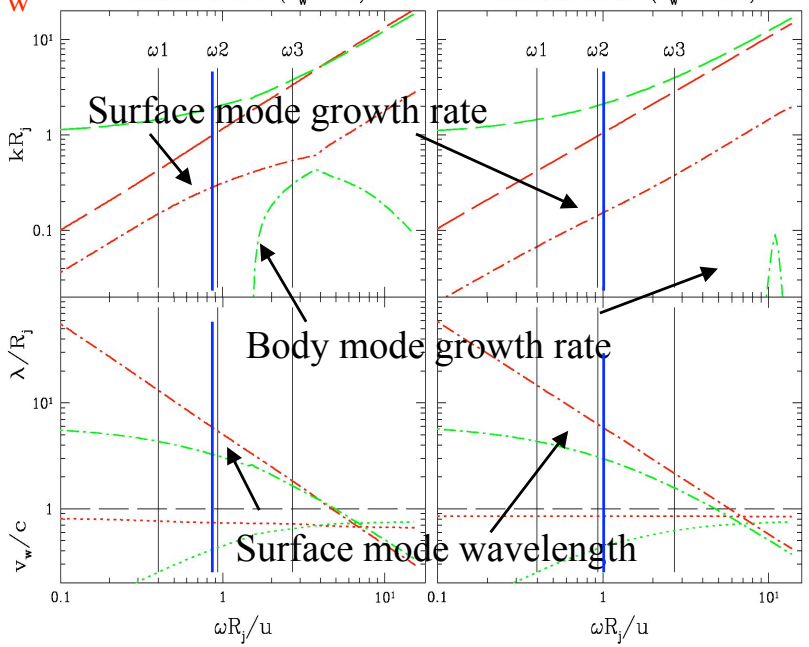

• A sheath with v_w = 0.5c significantly reduces the growth rate (red dash-dot) of the surface mode at simulation frequency ω2, and slightly increases the wavelength.
• Growth associated with the 1st helical body mode (green dash-dot) is almost eliminated by sheath flow.

3D RHD Jet Simulation Results at ω2

1D cut of radial velocity along jet

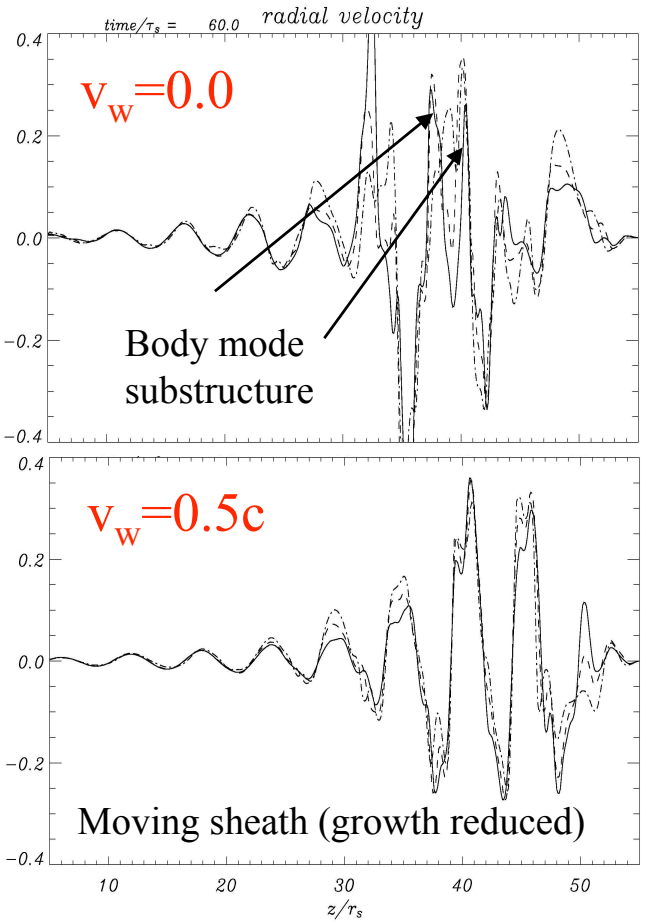

•The sheath wind reduces the growth rate and slightly increases the wave speed and wavelength as predicted.
• Substructure associated with the 1st helical body mode is eliminated by sheath wind as predicted.

3D RMHD Jet Simulations & Theory

3D RMHD Jet Simulation Results at ω2

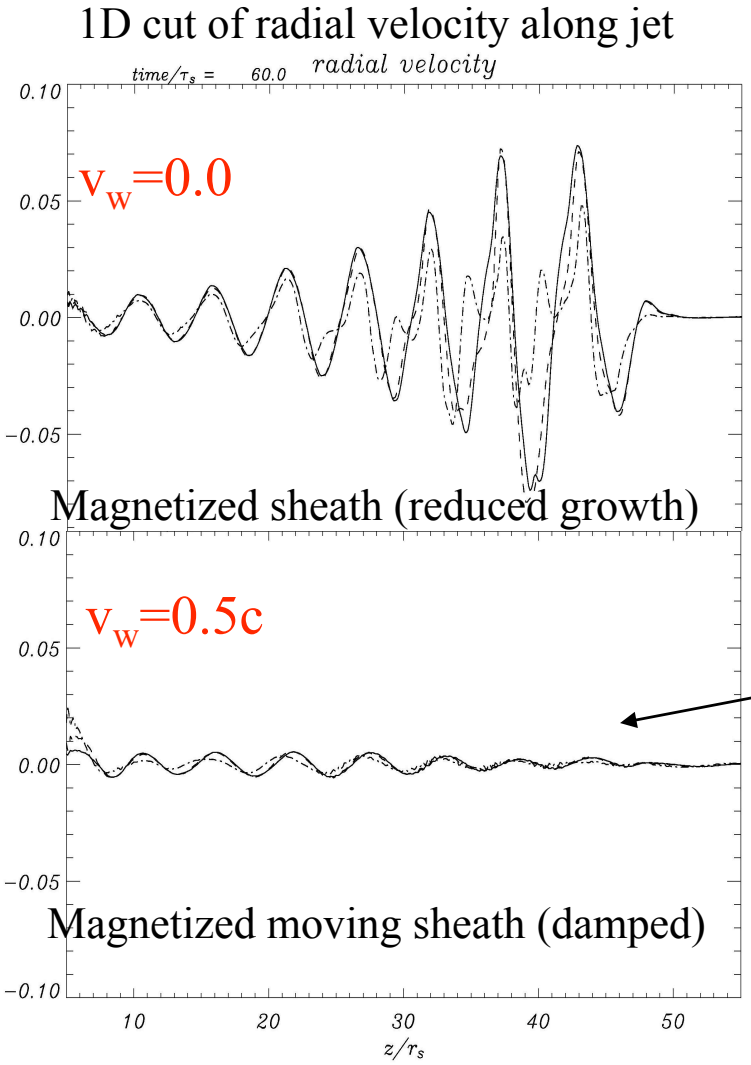

The magnetized sheath reduces growth rate relative to the fluid case and the magnetized sheath wind damped growth of KH modes.

Criterion for damped KH modes

Magnetized sheath flow has reduced the "velocity shear" to less than the "surface" Alfvén speed:

$$\gamma_j^2 \gamma_e^2 \left(u_j - u_e\right)^2 < V_{As}^2$$

Note that for comparable conditions in spine and sheath $V_{As} = 2\,\gamma_A\,(B^2/4\pi W)^{1/2}$ and $(B^2/4\pi W)^{1/2}$ can be >> c.

Stability Properties of Spine-Sheath Relativistic Jets

Hardee 2007

Dispersion Relation: $$\frac{\beta_j}{\chi_j}\frac{J_n'(\beta_j R)}{J_n(\beta_j R)} = \frac{\beta_e}{\chi_e}\frac{H_n^{(1)\prime}(\beta_e R)}{H_n^{(1)}(\beta_e R)}$$

J_n and $H_n^{(1)}$ are Bessel and Hankel functions and primes denote derivatives

$$\chi_j \equiv \gamma_j^2\gamma_{Aj}^2 W_j\left(\varpi_j^2 - \kappa_j^2 v_{Aj}^2\right) \qquad \chi_e \equiv \gamma_e^2\gamma_{Ae}^2 W_e\left(\varpi_e^2 - \kappa_e^2 v_{Ae}^2\right)$$

$$\beta_j^2 \equiv \left[\frac{\gamma_j^2\gamma_{Aj}^2\left(\varpi_j^2 - \kappa_j^2 a_j^2\right)\left(\varpi_j^2 - \kappa_j^2 v_{Aj}^2\right)}{\left(a_j^2 + \gamma_{Aj}^2 v_{Aj}^2\right)\varpi_j^2 - \gamma_{Aj}^2\kappa_j^2 v_{Aj}^2 a_j^2}\right] \qquad \beta_e^2 \equiv \left[\frac{\gamma_e^2\gamma_{Ae}^2\left(\varpi_{ex}^2 - \kappa_e^2 a_e^2\right)\left(\varpi_e^2 - \kappa_e^2 v_{Ae}^2\right)}{\left(a_e^2 + \gamma_{Ae}^2 v_{Ae}^2\right)\varpi_e^2 - \gamma_{Ae}^2\kappa_e^2 v_{Ae}^2 a_e^2}\right]$$

$$\varpi_{j,e}^2 \equiv \left(\omega - k u_{j,e}\right)^2 \qquad \kappa_{j,e}^2 \equiv \left(k - \omega u_{j,e}/c^2\right)^2$$

$$\gamma_{j,e} \equiv \left(1 - u_{j,e}^2/c^2\right)^{-1/2} \qquad \gamma_{sj,e} \equiv \left(1 - a_{j,e}^2/c^2\right)^{-1/2} \qquad \gamma_{Aj,e} \equiv \left(1 - v_{Aj,e}^2/c^2\right)^{-1/2}$$

$a = sound\ speed$ $\qquad$ $v_A = Alfven\ wave\ speed$

Surface Modes @ ω << ω*:

$$\frac{\omega}{k} = \frac{[\eta u_j + u_e] \pm i\eta^{1/2}\left[(u_j - u_e)^2 - V_{As}^2/\gamma_j^2\gamma_e^2\right]^{1/2}}{(1 + V_{Ae}^2/\gamma_e^2 c^2) + \eta(1 + V_{Aj}^2/\gamma_j^2 c^2)}$$

$$\eta \equiv \gamma_j^2 W_j/\gamma_e^2 W_e$$

$$V_{As}^2 \equiv \left(\gamma_{Aj}^2 W_j + \gamma_{Ae}^2 W_e\right)\frac{B_j^2 + B_e^2}{4\pi W_j W_e}$$

$$W_{j,e} \equiv \rho_{j,e} + [\Gamma/(\Gamma - 1)]P_{j,e}/c^2$$

Body Mode Condition:

$$\left[\frac{a_j^2 u_j^2 + \gamma_{Aj}^2 v_{Aj}^2(u_j^2 - a_j^2)}{\gamma_j^2\gamma_{Aj}^2(u_j^2 - a_j^2)(u_j^2 - v_{Aj}^2)}\right] > 0$$

Resonance (ω*) : $$\frac{u_j - u_e}{1 - u_j u_e/c^2} > \frac{v_{wj} + v_{we}}{1 + v_{wj}v_{we}/c^2}$$

$v_{wj} \equiv (a_j, v_{Aj})$ and $v_{we} \equiv (a_e, v_{Ae})$ in (fluid,magnetic) limits

$$v_w \approx v_w^* \equiv \frac{\gamma_j(\gamma_{we}v_{we})u_j + \gamma_e(\gamma_{wj}v_{wj})u_e}{\gamma_j(\gamma_{we}v_{we}) + \gamma_e(\gamma_{wj}v_{wj})}$$

$\gamma_{wj,e} \equiv (1 - v_{wj,e}^2/c^2)^{-1/2}$ for $v_{wj} \equiv (a_j, v_{Aj})$ and $v_{we} \equiv (a_e, v_{Ae})$ in (fluid,magnetic) limits

$$\omega R/v_{we} \approx \omega_{nm}^* R/v_{we} \equiv \frac{(2n+1)\pi/4 + m\pi}{\left[\left(1 - u_e/v_w^*\right)^2 - \left(v_{we}/v_w^* - u_e v_{we}/c^2\right)\right]^{1/2}}$$

$$\lambda_{nm}^* \equiv \frac{2\pi}{(2n+1)\pi/4 + m\pi}\left(\frac{\gamma_e}{v_{we}}\right)\left[\left(v_w^* - u_e\right)^2 - \left(v_{we} - (v_{we}u_e/c^2)v_w^*\right)^2\right]^{1/2} R$$

Growth Rate Reduction: Stability:

$$\gamma_j^2\gamma_e^2\left(u_j - u_e\right)^2 \longrightarrow \gamma_{Aj}^2\gamma_{Ae}^2\left(W_j/\gamma_{Ae}^2 + W_e/\gamma_{Aj}^2\right)\frac{B_j^2 + B_e^2}{4\pi W_j W_e}$$

$$\gamma_j^2\gamma_e^2\left(u_j - u_e\right)^2 < \gamma_{Aj}^2\gamma_{Ae}^2\left(W_j/\gamma_{Ae}^2 + W_e/\gamma_{Aj}^2\right)\frac{B_j^2 + B_e^2}{4\pi W_j W_e}$$

Resolution Test for CD kink Simulations

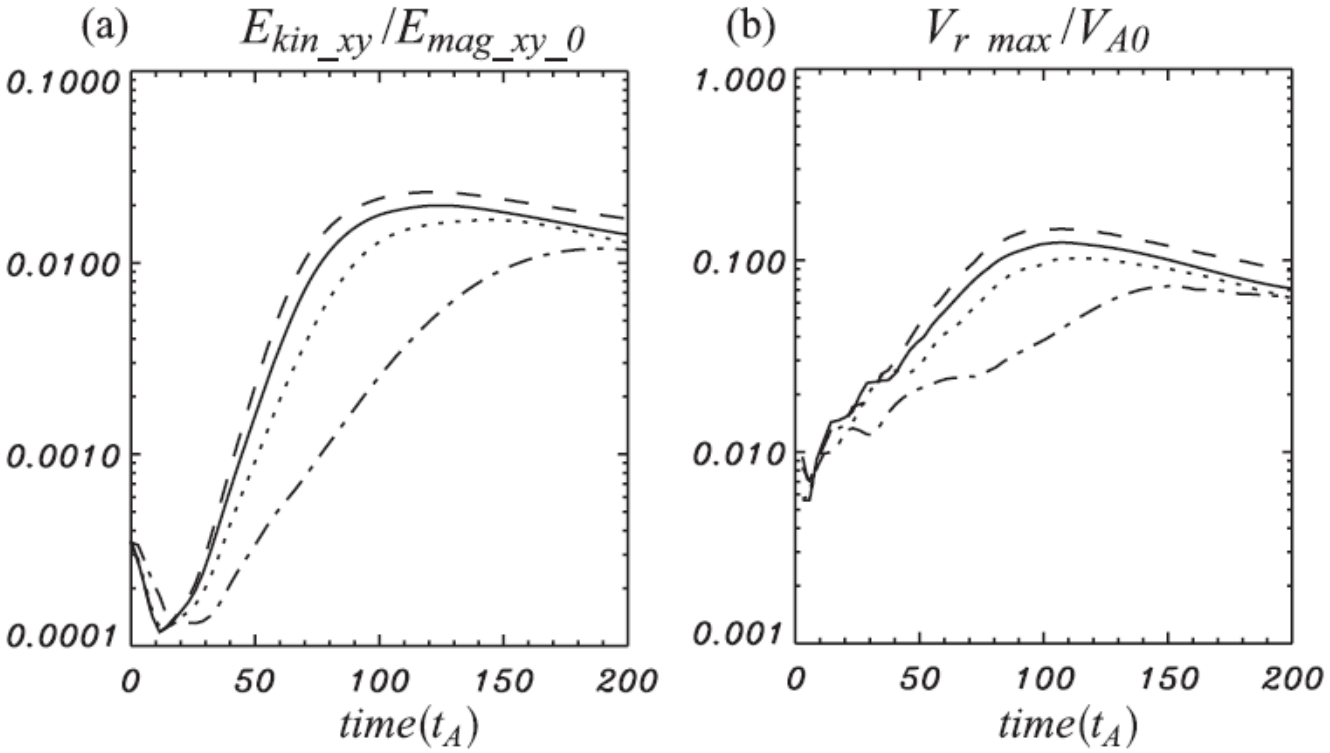

N/L=60 (dashed)
=40 (solid)
=30 (dotted)
=20 (dash-dotted)

- Higher resolution has faster growth rate and maximum amplitude
- Resolution of current simulation (*N/L=40*) is acceptable.

Dependence on Adiabatic Index for CD Kink Instability

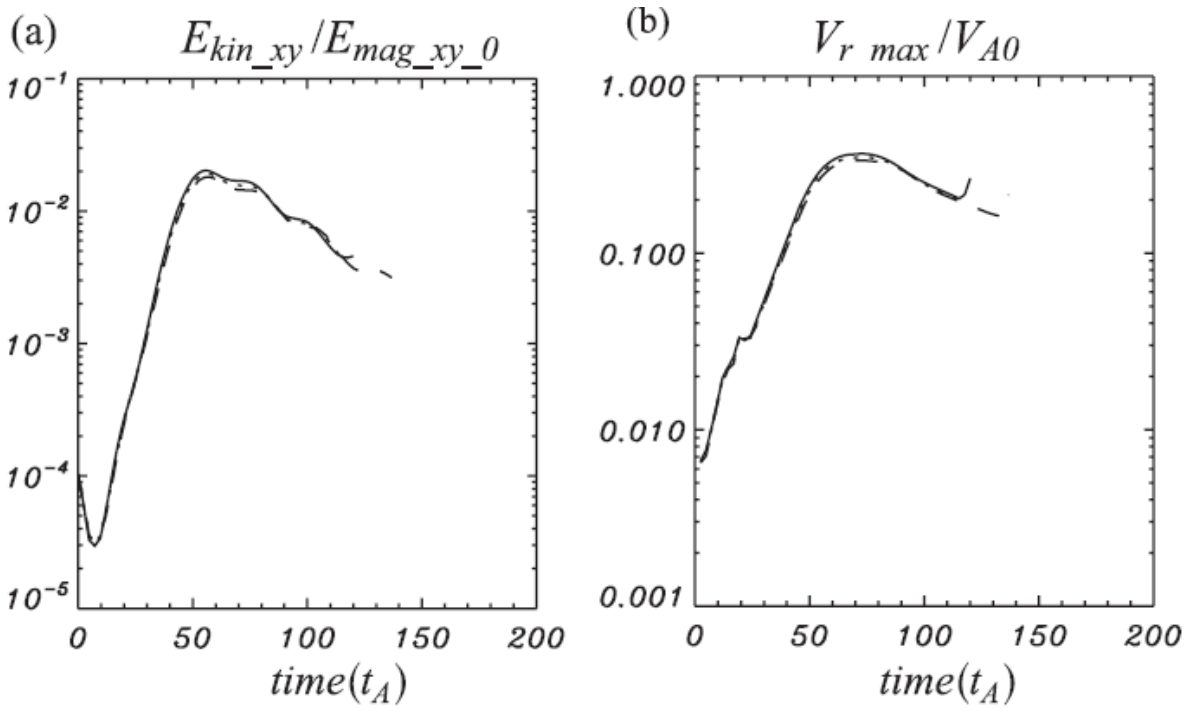

$\Gamma = 5/3$ (solid)
$= 13/9$ (dotted)
$= 4/3$ (dashed)

There are no difference between different adiabatic index

Non-relativistic CD Kink Instability

Appl et al. (2000)

- Consider force-free field with different radial pitch profile in the rest frame of jet

- maximum growth rate: $\Gamma_{max}=0.133\ v_A/P_0$, ($P_0=a$ in our notation)

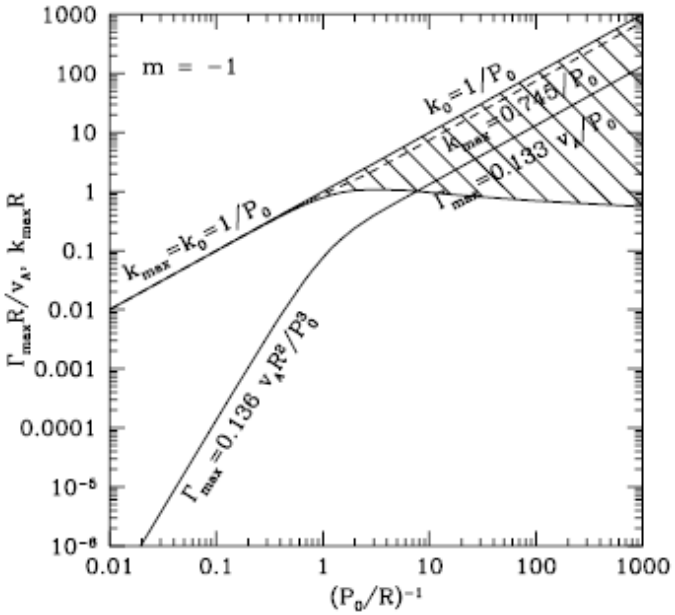

Maximum growth rate and unstable wave number for m=-1 kink as a function of characteristic radius of column

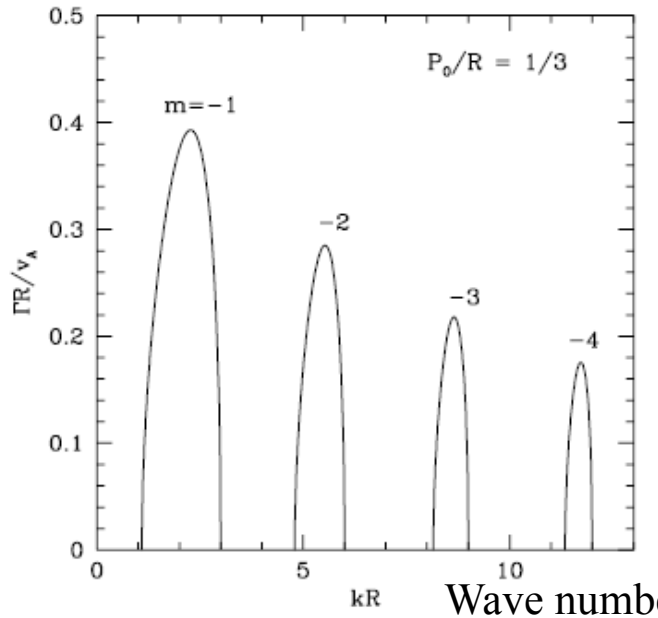

Wave number

Growth rate for m=-1~-4 in constant pitch case.

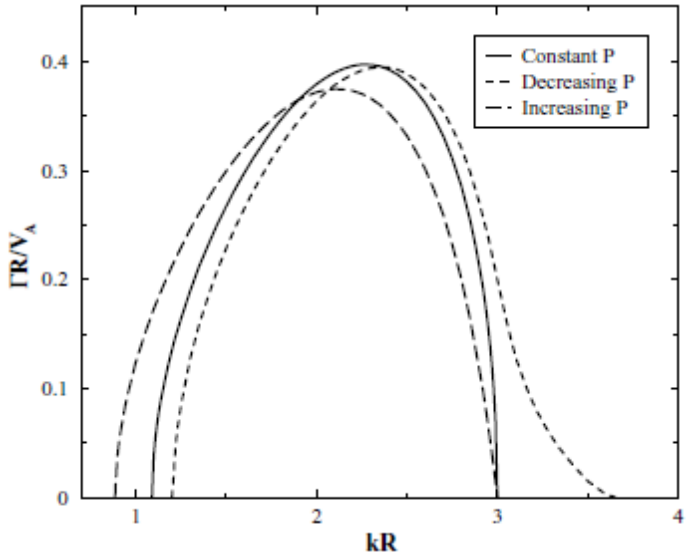

Growth rate for m=-1 mode as a function of wavenumber with different pitch profile